NAVAL POSTGRADUATE SCHOOL
Monterey, California

DTIC
ELECTE
MAR 0 7 1994
S B D

THESIS

EFFECT OF INITIAL IMPERFECTIONS ON THE
RESPONSE OF CYLINDERS TO UNDERWATER
EXPLOSION

by

Donald T. Hooker II

DECEMBER 1993

Thesis Advisor: Y. S. Shin

Approved for Public release: Distribution is unlimited

Best
Available
Copy

REPORT DOCUMENTATION PAGE		Form Approved OMB No. 0704

1. AGENCY USE ONLY	2. REPORT DATE 16 December, 1993	3. REPORT TYPE AND DATES COVERED Engineer's Thesis 10/92 to 12/93

4. TITLE AND SUBTITLE EFFECT OF INITIAL IMPERFECTIONS ON THE RESPONSE OF CYLINDERS TO UNDERWATER EXPLOSION

5. FUNDING NUMBERS

6. AUTHOR(S) D. T. Hooker II

7. PERFORMING ORGANIZATION NAME(S) AND ADDRESS(ES)
Naval Postgraduate School
Monterey, CA 93943-5000

8. PERFORMING ORGANIZATION REPORT NUMBER

9. SPONSORING/MONITORING AGENCY NAME(S) AND ADDRESS(ES)

10. SPONSORING/MONITORING AGENCY REPORT NUMBER

11. SUPPLEMENTARY NOTES The views expressed in this thesis are those of the author and do not reflect the official policy or position of the Department of Defense or the U.S. Government.

12a. DISTRIBUTION/AVAILABILITY STATEMENT Approved for public release: Distribution is unlimited.	12b. DISTRIBUTION CODE *A

13. ABSTRACT Presently, the United States Navy is searching for an improved method to predict the damage to a ship or underwater structure that results from an underwater explosion. One method of predicting this damage is through the use of nonlinear finite and boundary element analysis. Underwater Shock Analysis (USA) code combined with VEC/DYNA3D code is used for the analysis of the effect of explosive shock on numerical models. Initial geometric imperfections are introduced in the numerical model using modal imperfections. The resulting numerical model is then subjected to a simulated underwater shock using the combined USA/DYNA3D code. A sensitivity analysis is performed to look into the details on the damage resulting from these simulations.

14. SUBJECT TERMS UNDERWATER SHOCK, INITIAL IMPERFECTIONS			15. NUMBER OF PAGES 105
			16. PRICE CODE
17. SECURITY CLASSIFICATION OF REPORT Unclassified/Unlimited	18. SECURITY CLASSIFICATION OF THIS PAGE Unclassified	19. SECURITY CLASSIFICATION OF ABSTRACT Unclassified	20. LIMITATION OF ABSTRACT Unlimited

EFFECT OF INITIAL IMPERFECTIONS OF THE
RESPONSE OF CYLINDERS TO UNDERWATER EXPLOSION

by

Donald T. Hooker II
Lieutenant, United States Navy
B.S., The Ohio State University, 1979
M.S., Purdue University, 1981

Submitted in partial fulfillment of the
requirements for the degrees of

MASTER OF SCIENCE
IN MECHANICAL ENGINEERING
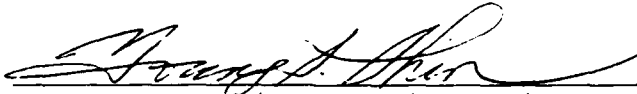and
MECHANICAL ENGINEER
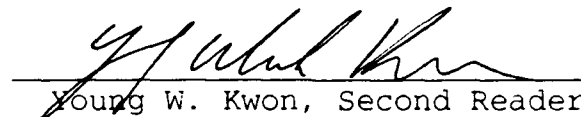
from the

NAVAL POSTGRADUATE SCHOOL
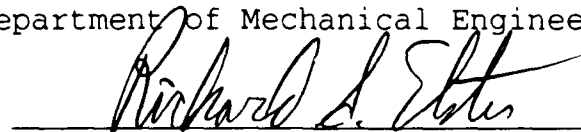December 1993

Author: _____
Donald T. Hooker II

Approved by: _____
Young S. Shin, Thesis Advisor

_____
Young W. Kwon, Second Reader

_____
Matthew D. Kelleher, Chairman
Department of Mechanical Engineering

_____
Richard S. Elster
Dean of Instruction

ABSTRACT

Presently, the United States Navy is searching for an improved method to predict the damage to a ship hull or underwater structure that results from an underwater explosion. One method of predicting this damage is through the use of nonlinear finite and boundary element analysis. Underwater Shock Analysis (USA) code combined with VEC/DYNA3D code is used for the analysis of the effect of explosive shock on numerical models. Initial geometric imperfections are introduced in the numerical model using modal imperfections. The resulting numerical model is then subjected to a simulated underwater shock using the combined USA/DYNA3D code. A sensitivity analysis is performed to look into the details on the damage resulting from these simulations.

iii

TABLE OF CONTENTS

iv

ACKNOWLEDGMENTS

I. INTRODUCTION

The use of USA/DYNA3D for analyzing structures subjected to underwater shock has been shown to be an effective tool in predicting the response of these structures and the resulting damage (Chisum 1992). In some cases the actual deformation of a cylinder subjected to an underwater shock is not accurately predicted. One explanation for this inaccuracy is that actual cylinders have many imperfections (e.g., out of roundness, thin sections, voids, etc.) and the finite element modeling of these cylinders often do not take into account the initial imperfections that are present. By introducing imperfections in the position of the node points generated by a finite element mesh generator it is possible to more accurately model the geometry of an actual cylinder. With a more accurate model of the actual cylinder the finite element numerical analysis of the resulting damage due to underwater shock may be more accurate as well.

II. INITIAL IMPERFECTIONS

The location of the node points of a structure modeled by a finite element mesh generator are precisely located (to the numerical accuracy of the modeling code) at the positions specified in the inputs to the mesh generator algorithm. Manufactured structures usually have many imperfections that are not accurately modeled by many finite element mesh generators. Surveys have been performed to measure the imperfections that naturally exist in cylindrical shell structures (Arbocz 1982). These data have been collected into data banks, and Arbocz suggests that they be used to improve design criteria for buckling of thin shells. The imperfection data banks show that imperfections have characteristic distributions that include decreasing modal amplitudes with increasing mode number. Kirkpatrick (1989) found that by introducing initial modal imperfections in a cylindrical structure subjected to blast shock loading that the resulting numerical analysis agreed much closer to the experimental data than the analysis without these initial imperfections.

Initial imperfections were introduced into the location of the node points of the finite element model using a

summation of modal imperfections expressed as the cosine series shown in Eq. (1).

$$\Delta R(\theta) = \sum_{n=2}^{N} A_n \cos(n\theta + \phi_n) \quad \ldots \ldots \ldots \ldots \quad (1)$$

where ΔR is the radial imperfection, θ is the angular position, N is the maximum modal contribution, A_n is the modal amplitude, and ϕ_n is a random modal phase shift. The assumption that the modal phase shift is a random variable is reasonable for many shells. An empirical form for the modal amplitude is expressed as shown in Eq. (2).

$$A_n = \frac{X}{n^r} \quad \ldots \ldots \ldots \ldots \ldots \ldots \ldots \quad (2)$$

where A_n is the modal amplitude of the nth modal imperfection, n is the mode number and X and r are coefficients used to fit the available data for shells of a given construction. The modal amplitude can be modeled as a constant percentage of the shell thickness. For many of the studies in this investigation the modal amplitude is constant as shown in Eq. (3) at 1% of the shell thickness for all modes.

$$A_n = 0.01h \qquad \text{for all } n \quad \ldots \ldots \ldots \ldots \quad (3)$$

Kirkpatrick found that the modal amplitudes in Eq. (4) and (5) accurately modeled the imperfections of his test cylinder.

$$A_n = 0.05h \qquad\qquad n \leq 6 \quad \ldots \ldots \ldots \ldots \ldots \ldots \ldots (4)$$

$$A_n = \frac{2h}{n^2} \qquad\qquad n \geq 7 \quad \ldots \ldots \ldots \ldots \ldots \ldots (5)$$

The modal imperfections introduced in this study are assumed to be a function only of the circumferential position of the node and not a function of the axial position of the node. The programs used to modify the node positions are shown in Appendix A.

III. TWO DIMENSIONAL INFINITE CYLINDER MODELS

Fox (1992) developed a two dimensional infinite cylinder model to validate the use of the USA/DYNA3D code for use in underwater shock analysis. This model was further developed into the full symmetry two dimensional infinite cylinder model shown in Figure 1. This model has 40 elements around the circumference of the cylinder, radius of 6 inches, shell thickness of 0.06 inches and an element length of 0.006 inches. The same restriction on the length of the elements found for the model Fox developed (length/radius=0.001) was also true for this model. Fox stated that longer elements resulted in "residual three dimensional effects" that caused oscillations in the numerical results. Symmetric boundary conditions were imposed on both ends of the cylinder to model an infinite length cylinder. This model and all subsequent models (unless specifically noted) use Belytschko-Tsay (Belytschko 1984) shell elements for their numerical efficiency and to eliminate the problems of using a solid element to model a thin walled structure. For details of the model input parameters see Appendix B. The shell material is modeled as mild steel, an elastic-plastic material with a Young's modulus of 2.9×10^7 psi, a Poisson's ratio of 0.3, a
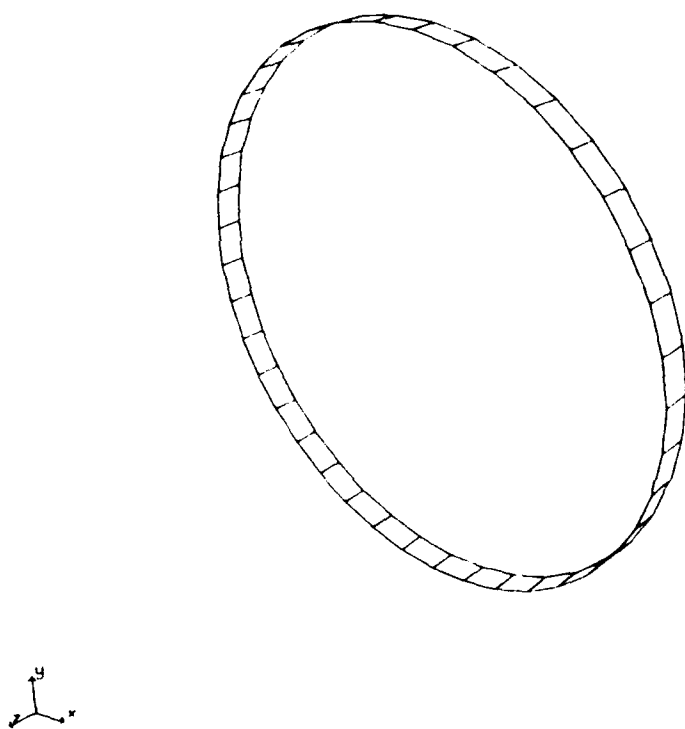
5

Figure 1.   Two Dimensional Infinite Cylinder Model

hardening modulus of 5100 psi and a yield stress of 32,000 psi. For details of the material models used in this study see Appendix C.

A. Perfect Cylinder Model

This cylinder was subjected to a underwater shock wave modeled as a plane wave with an amplitude of 500 psi and a duration of 1 millisecond resulting from an explosive charge located along the x-axis. The pressure time history of the shock wave is shown in Figure 2. The early damage pattern of the cylinder at 0.5 milliseconds is shown in Figure 3. The front face of the cylinder is flattened by the impacting plane wave approaching from the right. However, Figure 4 shows that the final damage pattern at 5 milliseconds is very different than this early deformation pattern. All plastic deformation has been completed by 5 milliseconds. The side of the cylinder facing the approaching shock wave shows a pronounced protrusion. This pattern was unexpected based on experimental results which have usually shown inward deformations of a cylindrical shell facing the explosive charge. It is hypothesized that this raised section is due to the fact that the modeled cylinder is a perfect cylinder and is not representative of a true manufactured cylinder. The manufactured cylinder will have
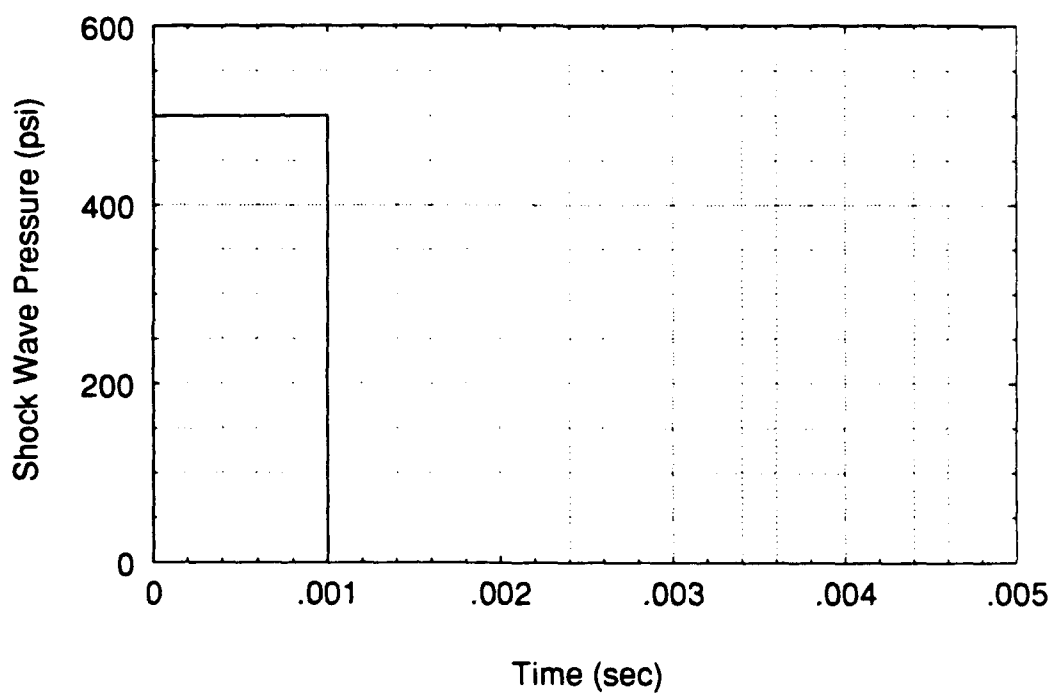
7

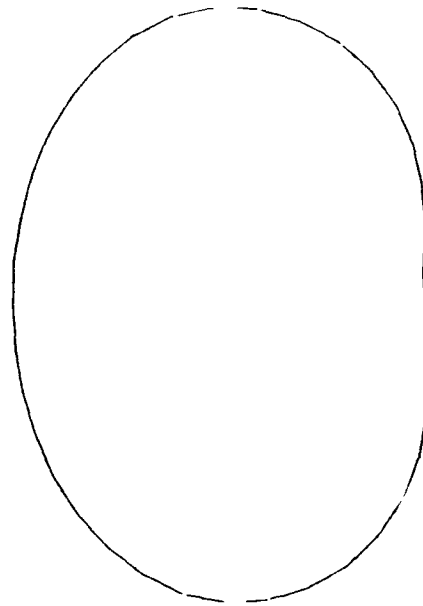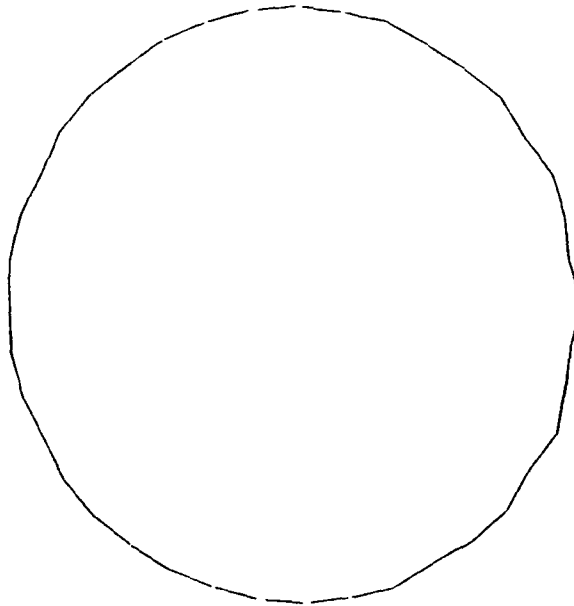Figure 2.   Pressure Time History of 500 psi 1 ms Shock Wave

8

←Shock
Wave

0.5 ms (deformations scaled up 100X)

Figure 3. Deformation of Two Dimensional Infinite Cylinder
Subjected to a Square Pressure Pulse of 500 psi for 1 ms
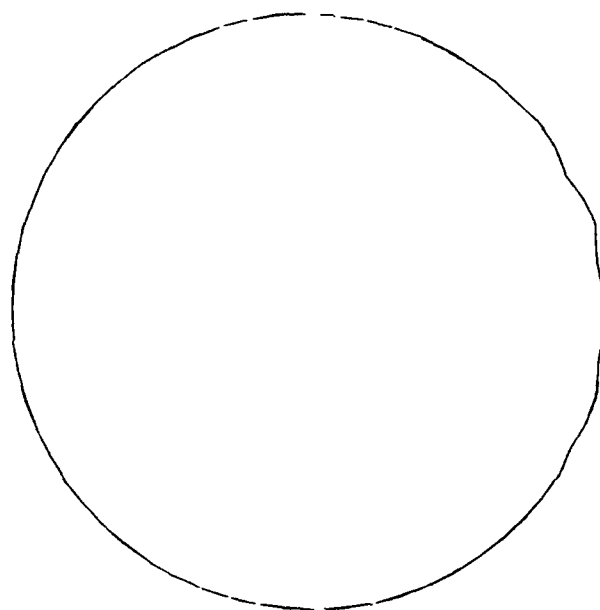
←Shock
Wave

5.0 ms (deformations scaled up 10X)

Figure 4. Deformation of Two Dimensional Infinite Cylinder
Subjected to a Square Pressure Pulse of 500 psi for 1 ms

9

many imperfections in the shell which is not present in the computer models.

In order to study the effect of mesh size on the response of this cylinder another model was developed with 64 elements around the circumference of the cylinder. Figure 5 shows that the response of this cylinder is similar to that for the 40 element cylinder. There is still a distinct protrusion of the shell toward the direction of the approaching shock wave. All subsequent cylinders will use 40 elements around the circumference of the cylinder.

## B. Imperfect Cylinder Models

The introduction of initial imperfections significantly changes both the shape and magnitude of the resulting deformation. Introduction of a 6th mode imperfection, as shown in Figure 6 (imperfection magnitude scaled by a factor of 100) with a modal amplitude of 5% of the shell thickness and no random phase shift, results in the damage pattern shown (deformations scaled by factor of 10) in Figure 7. A mode 6 imperfection was chosen because of the ease in identifying its distinctive pattern. Use of another model imperfection would only have changed the shape of the final deformation not any conclusions resulting from this study. Comparison of the final damage pattern with the shape of the initial imperfection shows that the damage pattern follows

←Shock
Wave

5.0 ms (deformations scaled up 10X)

Figure 5.   Deformation of Two Dimensional Infinite Cylinder
Subjected to a Square Pressure Pulse of 500 psi for 1 ms
Fine Mesh
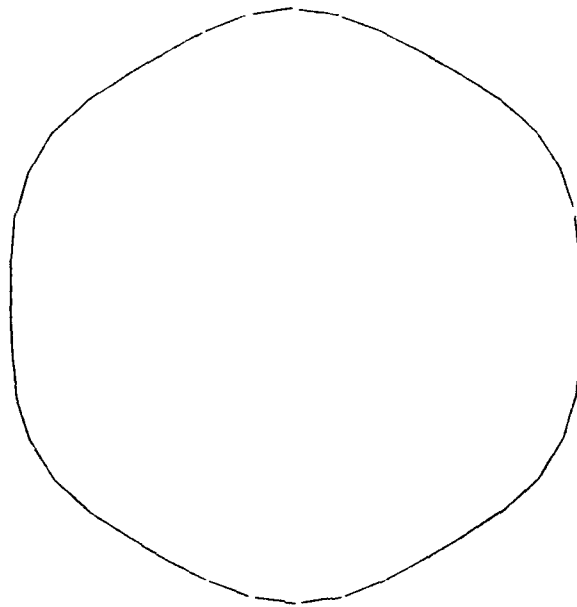
Initial Mode 6 Imperfection (imperfections scaled up 100X)

Figure 6. Two Dimensional Infinite Cylinder Subjected to a Square Pressure Pulse of 500 psi for 1 ms, Mode 6 Initial Imperfection $A_6 = 0.05h$ no phase shift
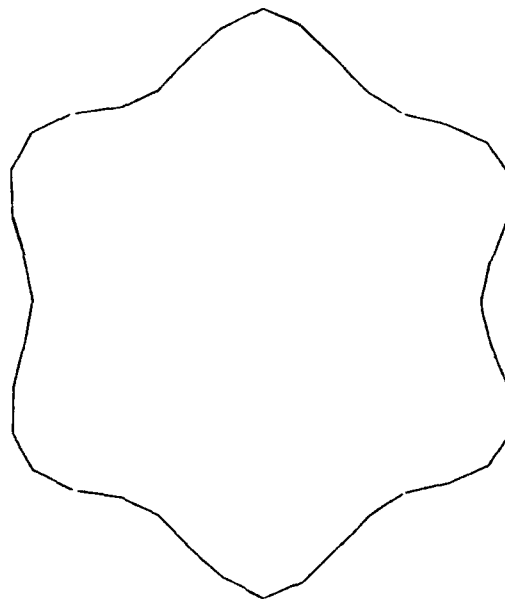

←Shock Wave

5.0 ms (deformations scaled up 10X)

Figure 7. Two Dimensional Infinite Cylinder Subjected to a Square Pressure Pulse of 500 psi for 1 ms, Mode 6 Initial Imperfection $A_6 = 0.05h$ no phase shift

12

the initial imperfection resulting in a final damage pattern looking like the mode 6 initial imperfection magnified due to the external shock wave applied to the cylinder. The introduction of imperfections caused the deformation of the cylindrical shell to follow the initial imperfection pattern of the shell. In addition to changing the damage pattern, the initial imperfection also causes much greater deflections of the shell for the same shock wave intensity. Figure 8 shows the deformation of a two dimensional cylinder with an initial imperfection 5% of the shell thickness with only a mode 10 contribution and no random phase shift. Comparison of Figures 7 and 8 show that increasing the mode number of the initial imperfection while keeping the amplitude constant at 5% of the shell thickness results in greater damage to the cylinder for the same shock wave pressure. This is due to the greater local curvature of the shell with imperfections of higher mode number than for lower mode numbers. Figure 9 shows how the total internal strain energy (a measure of the damage to the cylinder) of the cylinders increases as the mode number of the initial imperfection increases while the amplitude of the imperfection is constant at 5% of the shell thickness for the same shock wave pressure.

Another cylinder was modeled with imperfections containing the first 10 modal imperfections, as shown in
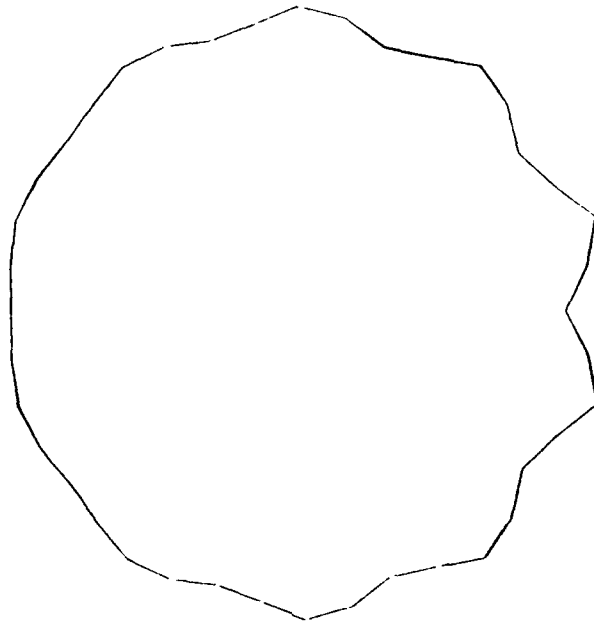
5.0 ms (deformations scaled up 3X)

Figure 8.   Two Dimensional Infinite Cylinder Subjected to a
Square Pressure Pulse of 500 psi for 1 ms, Mode 10 Initial
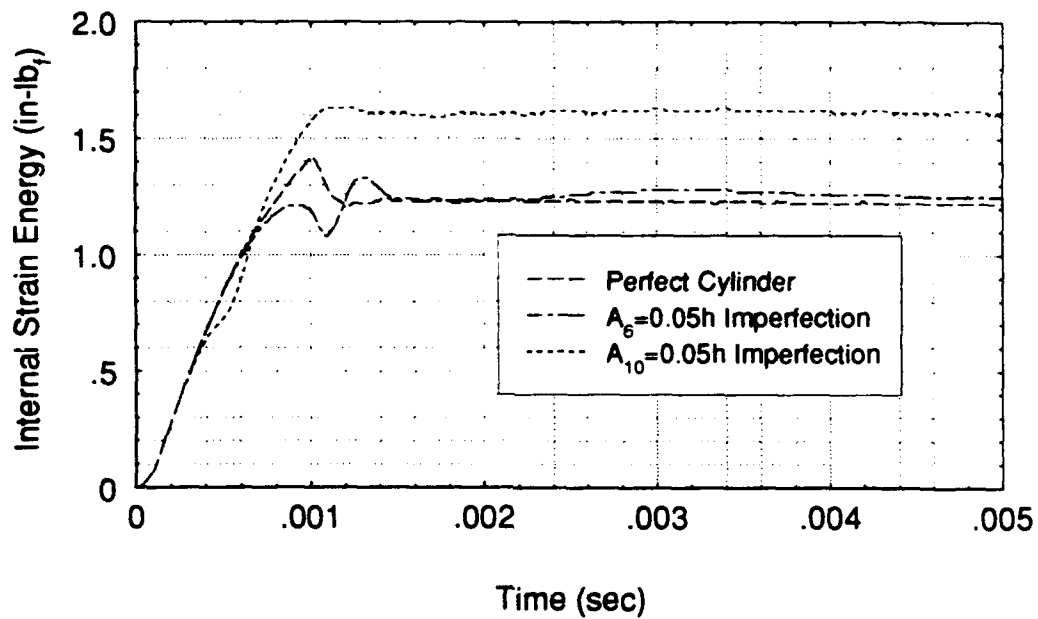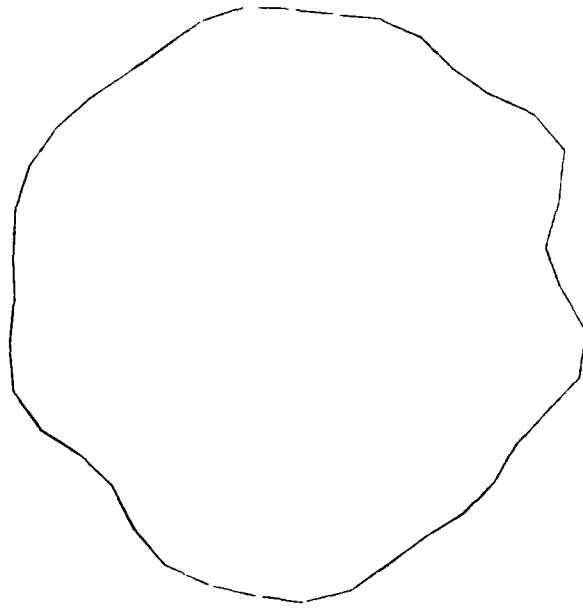Imperfection $A_{10}=0.05h$ no phase shift

Figure 9.   Total Internal Strain Energy for Cylinders
subjected to a Square Pressure Pulse of 500 psi for 1 ms

14

Figure 10 with modal amplitudes for each mode of 1% of the shell thickness and with random phase shifts. The resulting damage pattern is shown in Figure 11. Again, the general shape of the final deformation pattern is very close to the shape of the initial imperfection pattern.

The introduction of a different initial imperfection, shown in Figure 12 with initial imperfections magnified by 50 times, using the modal amplitude of equations (4) and (5), results in the final deformation pattern shown in Figure 13. Again, the deformation of the shell of the cylinder follows the initial imperfection pattern.

Initial Imperfection (imperfections scaled up 200X)

Figure 10. Two Dimensional Infinite Cylinder Subjected to a
Square Pressure Pulse of 500 psi for 1 ms, Initial
Imperfection First 10 Modes $A_n = 0.01h$ with Random Phase Shift
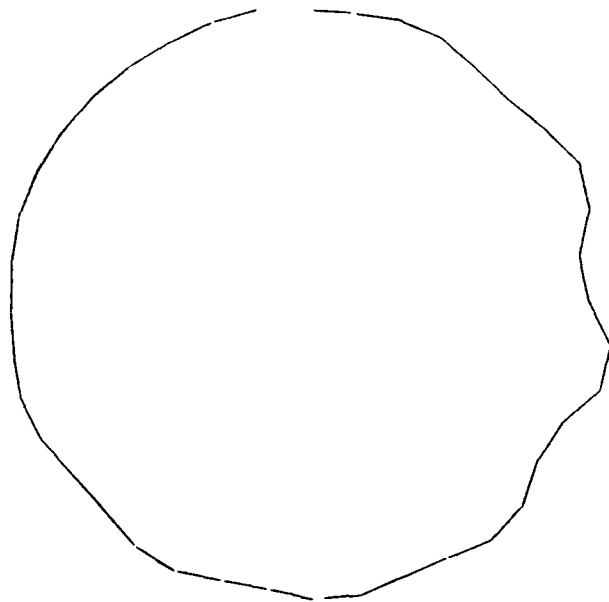
←Shock
Wave

5.0 ms (deformations scaled up 2X)

Figure 11. Two Dimensional Infinite Cylinder Subjected to a
Square Pressure Pulse of 500 psi for 1 ms, Initial
Imperfection First 10 Modes $A_n = 0.01h$ with Random Phase Shift

16

Initial Imperfection (imperfections scaled up 50X)

Figure 12. Two Dimensional Infinite Cylinder Subjected to a Square Pressure Pulse of 500 psi 1 ms, Initial Imperfection First 10 modes $A_n = 0.05h$ for Modes 2 through 6, $A_n = 2h/n^2$ for Modes 7 through 10 with Random Phase Shift
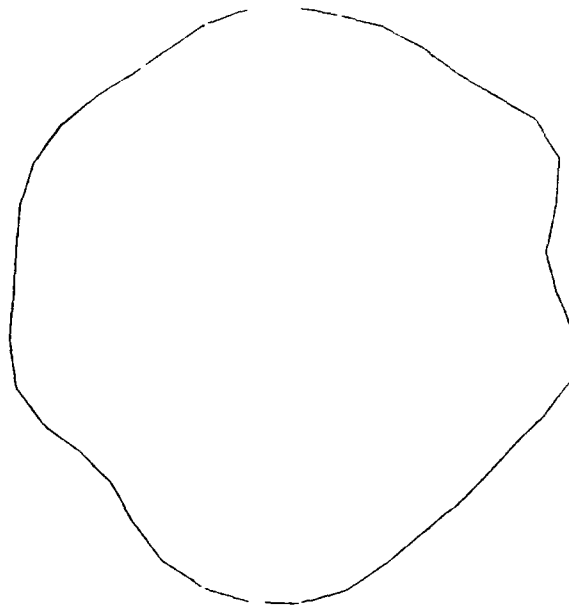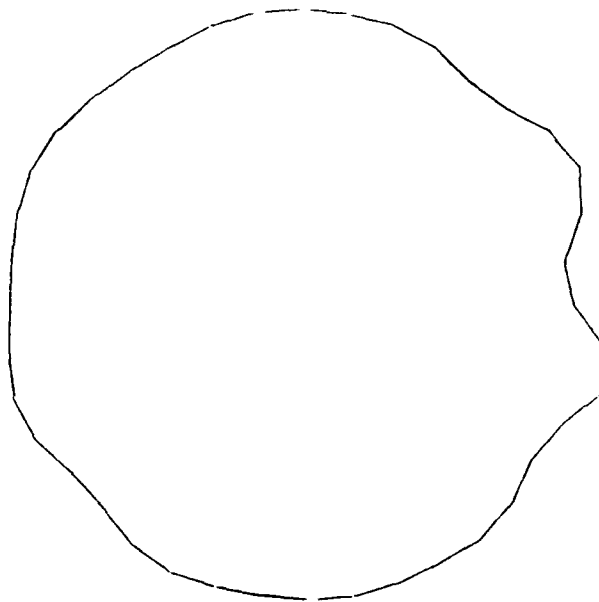

←Shock
Wave

5.0 ms (deformations scaled up 2X)

Figure 13. Two Dimensional Infinite Cylinder Subjected to a Square Pressure Pulse of 500 psi 1 ms, Initial Imperfection First 10 modes $A_n = 0.05h$ for Modes 2 through 6, $A_n = 2h/n^2$ for Modes 7 through 10 with Random Phase Shift

17

IV. THREE DIMENSIONAL RING STIFFENED INFINITE CYLINDER MODELS

The three-dimensional ring stiffened infinite cylinder model shown in Figure 14 was developed from the two-dimensional infinite cylinder model. This model has a total of 400 elements with 40 elements in the circumferential direction and 10 elements along the length. Again symmetric boundary conditions were imposed on both ends of the cylinder to model an infinite cylinder. This three-dimensional model has stiffeners 0.12 inches thick and 1 inch deep located on 12 inch spacing. The shell is 0.06 inches thick. For details in the model input parameters see Appendix D The shell and stiffeners are modeled as mild steel with the same properties as listed earlier

A. Perfect Cylinder Model

This cylinder was subjected to the same plane shock wave as the previous models. The early deformation of the cylinder at 0.2 milliseconds (Figure 15) shows the outer shell pinching in on either side of the stiffener located in the center of the cylinder. Figure 16 shows the flattening of the face of the cylinder facing the explosive charge at 0.2 milliseconds. At this time in the deformation history

18
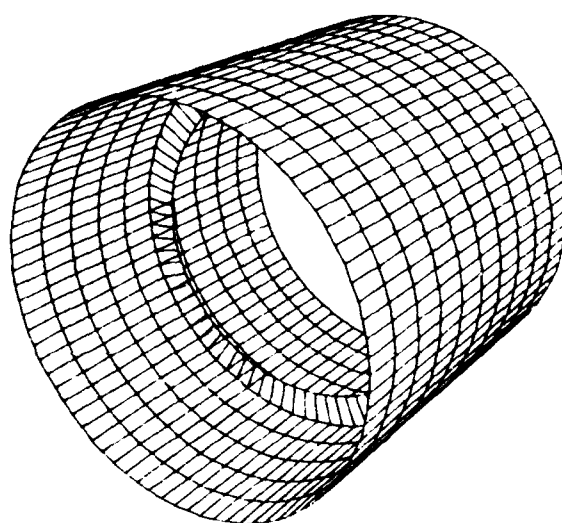
Figure 14. Three Dimensional Ring Stiffened Infinite
Cylinder Model
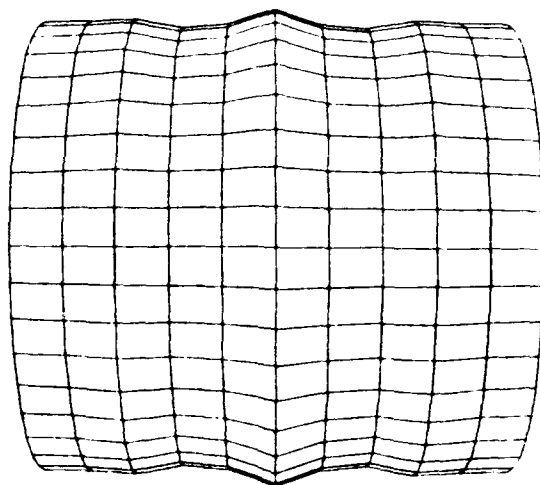
Front View @ 0.2 ms (deformations scaled up 50X)

Figure 15. Deformation of Three Dimensional Ring Stiffened
Infinite Length Cylinder Subjected to a Square Pressure
Pulse of 500 psi for 1 ms
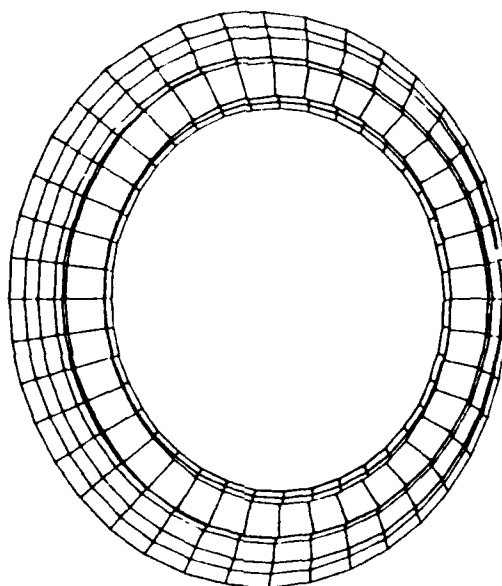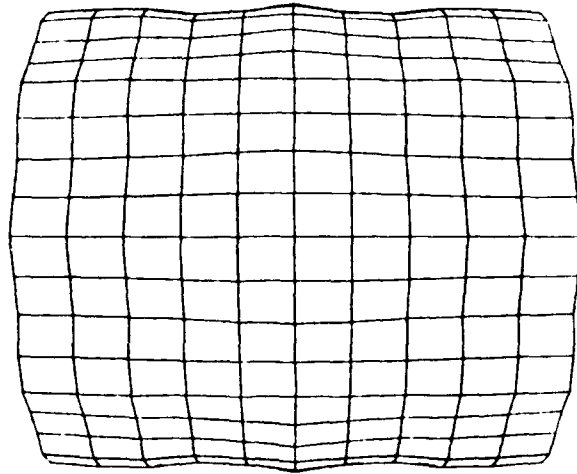

←Shock
Wave

End View @ 0.2 ms (deformations scale up 50X)

Figure 16. Deformation of Three Dimensional Ring Stiffened
Infinite Length Cylinder Subjected to a Square Pressure
Pulse of 500 psi for 1 ms

there is no evidence of the formation of a local raised area on the front of the cylinder facing the charge. The final deformation pattern shown in Figure 17 shows pinching of the shell on either side of the stiffener. This pinching effect was also noted by Chisum (1992) and appears to be present in many finite element simulations of underwater shock which model test cylinders as perfect cylinders. Again, the final deformation pattern of the cylinder side facing the charge has a local protrusion of the shell material toward the explosive charge as shown in Figure 18. Again, it is hypothesized that this damage pattern is the result of the model cylinder being a perfect cylinder while test cylinders will always have imperfections in the shell of the cylinder.

B. Imperfect Cylinder Models

The introduction of initial imperfections significantly changes both the shape and magnitude of the final deformations seen in this cylinder model. The 5% mode 6 imperfection shown in Figure 19 was introduced into this model. The resulting deformation due to a 500 psi 1 millisecond plane wave pressure pulse is shown in Figures 20 through 23. The initial imperfection shape is clearly evident in the final damage pattern. However the shape of the cylinder at 0.2 milliseconds does not show any of the initial imperfection. There is insufficient time elapsed

21

Front View @ 5.0 ms

Figure 17. Deformation of Three Dimensional Ring Stiffened
Infinite Length Cylinder Subjected to a Square Pressure
Pulse of 500 psi for 1 ms
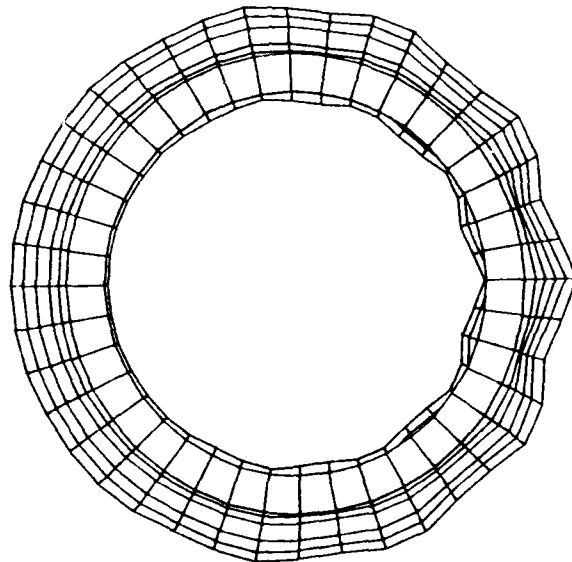
←Shock
Wave

End View @ 5.0 ms

Figure 18. Deformation of Three Dimensional Ring Stiffened
Infinite Length Cylinder Subjected to a Square Pressure
Pulse of 500 psi for 1 ms

22

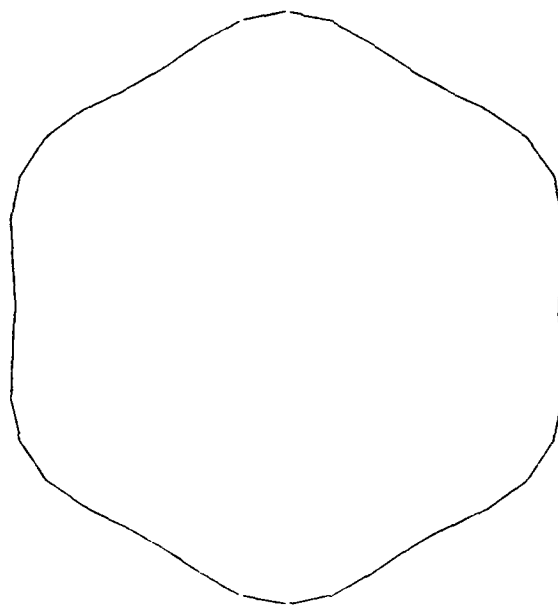Mode 6 Initial Imperfection $A_6 = 0.05h$ no phase shift
(imperfections scaled up 100X)

Figure 19.   Deformation of Three Dimensional Ring Stiffened
Infinite Length Cylinder Subjected to a Square Pressure
Pulse of 500 psi for 1 ms
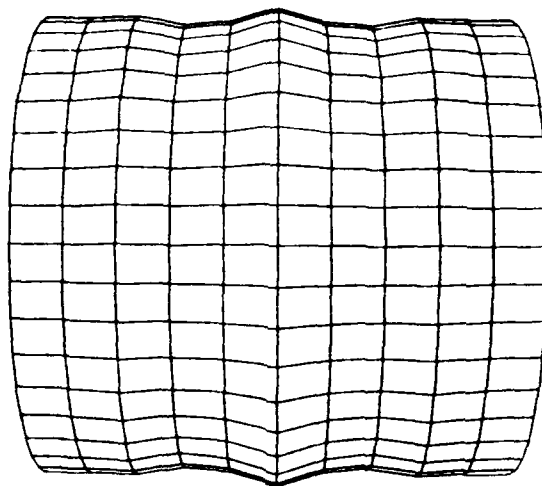
Front View @ 0.2 ms (deformations scaled up 50X)

Figure 20.   Deformation of Three Dimensional Ring Stiffened
Infinite Length Cylinder with a Mode 6 Initial Imperfection
$A_6 = 0.05h$ no phase shift, Subjected to a Square Pressure
Pulse of 500 psi for 1 ms
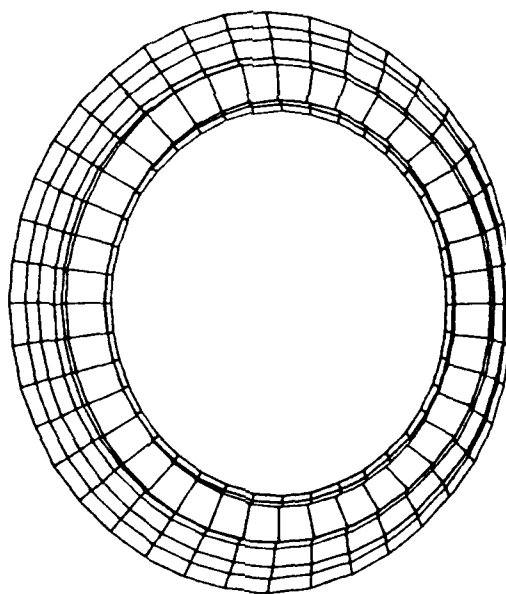
←Shock
Wave

End View @ 0.2 ms (deformations scaled up 50X)

Figure 21.   Deformation of Three Dimensional Ring Stiffened
Infinite Length Cylinder with a Mode 6 Initial Imperfection
$A_6 = 0.05h$ no phase shift, Subjected to a Square Pressure
Pulse of 500 psi for 1 ms

Front View @ 5.0 ms

Figure 22. Deformation of Three Dimensional Ring Stiffened
Infinite Length Cylinder with a Mode 6 Initial Imperfection
$A_6 = 0.05h$ no phase shift, Subjected to a Square Pressure
Pulse of 500 psi for 1 ms

←Shock
Wave

End View @ 5.0 ms

Figure 23. Deformation of Three Dimensional Ring Stiffened
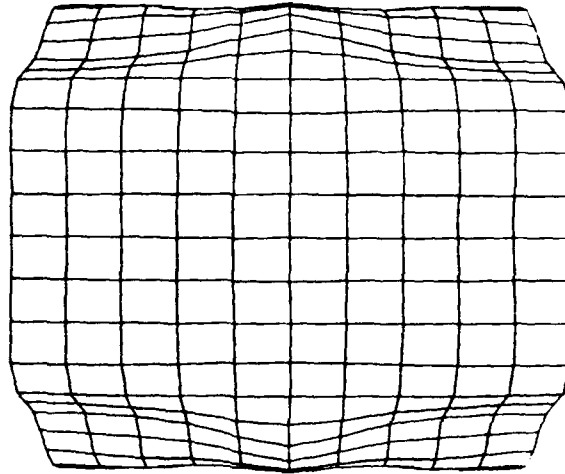Infinite Length Cylinder with a Mode 6 Initial Imperfection
$A_6 = 0.05h$ no phase shift, Subjected to a Square Pressure
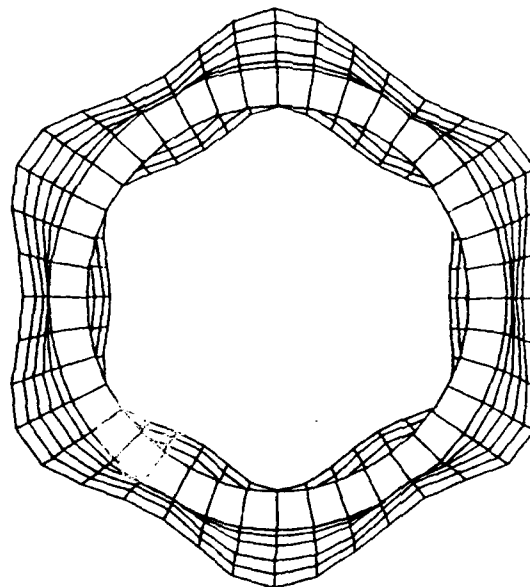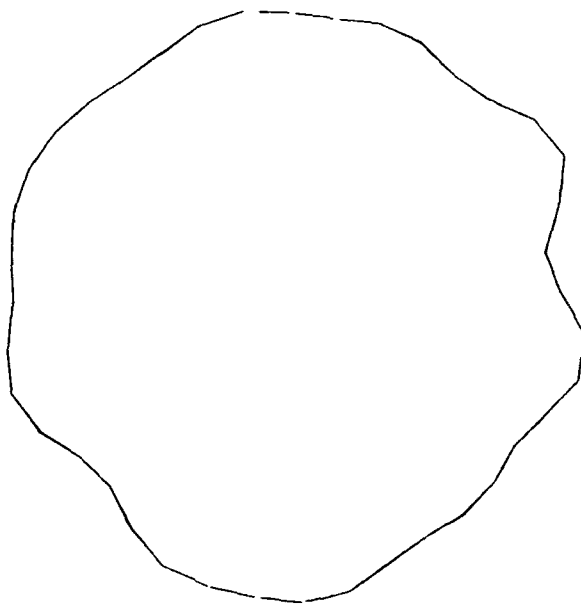Pulse of 500 psi for 1 ms

for the deformations to grow large enough to show this initial imperfection. However the pinching of the shell on either side of the stiffener has already begun at 0.2 milliseconds. The final deformation still shows this pinching effect however the magnitude of this type of deformation is reduced by the initial imperfection.

With the introduction of an initial imperfection of the first 10 modes with modal amplitudes of 1% of the shell thickness and with random phase shifts as shown in Figure 24 the resulting damage pattern again shows that the deformation of the shell will preferentially follow the initial imperfections. The resulting damage pattern is very different from the perfect case (Figures 25 and 26). Most noteworthy is the elimination of the pinch in the outer shell on either side of the stiffener. In addition the magnitude of the deformation in the outer shell is much greater than for the perfect cylinder case. The introduction of these imperfections results in sites where the cylinder preferentially deforms during the shock pressure. Thus when the cylinder deforms the deformation follows the initial imperfections resulting in the final shape of the cylinder looking like the initial imperfection shape.

Initial Imperfection (imperfections scaled up 200X)

Figure 24. Three Dimensional Ring Stiffened Infinite Length
Cylinder Subjected to a Square Pressure Pulse of 500 psi for
1 ms, Initial Imperfection First 10 Modes $A_n = 0.01h$ with
Random Phase Shift

27
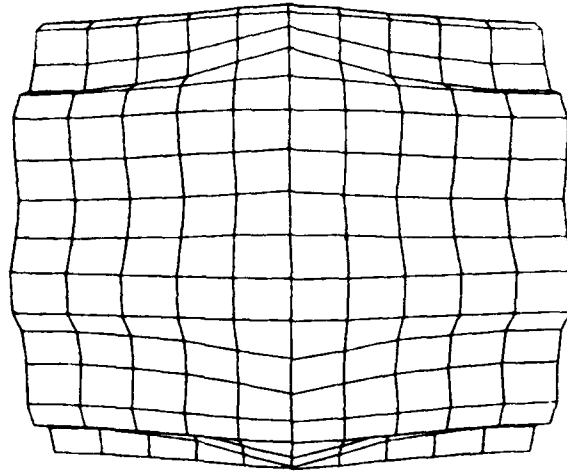
Front View @ 5.0 ms

Figure 25. Three Dimensional Ring Stiffened Infinite Length
Cylinder Subjected to a Square Pressure Pulse of 500 psi for
1 ms, Initial Imperfection First 10 Modes $A_n = 0.01h$ with
Random Phase Shift
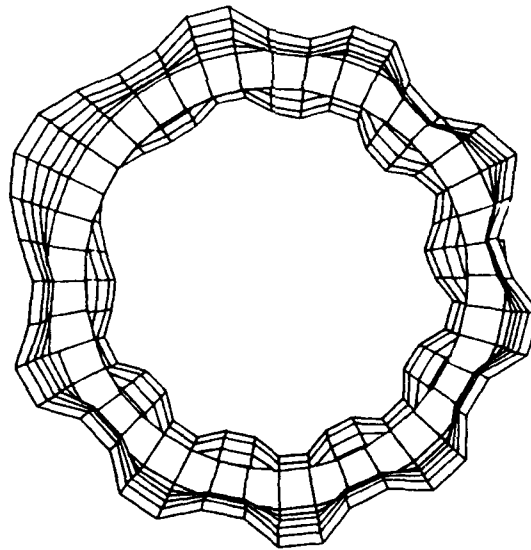
←Shock
Wave

End View @ 5..0 ms

Figure 26. Three Dimensional Ring Stiffened Infinite Length
Cylinder Subjected to a Square Pressure Pulse of 500 psi for
1 ms, Initial Imperfection First 10 Modes $A_n = 0.01h$ with
Random Phase Shift

C. Parametric Study on the Effect of Cylinder Geometry

A parametric study changing basic cylinder geometry was done to see the effect of these changes on the response of a three dimensional ring stiffened infinite cylinder to underwater shock. The parameters were varied as follows:

Shell Thickness   0.06, 0.12 and 0.24 inches
Stiffener Spacing   12.0, 8.0 and 6.0 inches
Diameter   8.0, 12.0 and 18.0 inches

This geometric variation covers the range of shell thickness to radius ratios from 0.0067 to 0.06 and stiffener spacing to radius ratios from 0.67 to 3.0.

Increasing the shell thickness strengthened the cylinders and in order to obtain significant permanent deformation of the shell it was necessary to increase the amplitude of the input shock wave. The amplitude of the shock wave was adjusted to cause damage to the cylinder without completely collapsing the cylinder. This input shock wave pressure ranged from 500 psi for 1 ms for the thinnest shell to 2400 psi for 1 ms for the thickest shell.

The resulting damage patterns for a perfect cylinder 8.0 inches in diameter (shell thickness to radius ratios from 0.015 to 0.06 and stiffener spacing to radius ratios from 1.5 to 3.0) are shown in Figures 27 and 28. The shock wave pressure for the 0.06 inch shell thickness is 600 psi for 1 ms, for the 0.12 inch shell thickness the pressure is

29

1200 psi for 1 ms and for the 0.24 inch shell thickness the pressure is 2400 psi for 1 ms.

The front view shows that increasing the shell thickness causes the pinching of the shell near the stiffener to decrease but it is not entirely eliminated at a shell thickness of 0.24 inches. Decreasing the stiffener spacing to 8.0 inches from 12.0 inches also has little effect on the pinching of the shell but at a stiffener spacing of 6.0 inches there is very little pinching of the shell near the stiffener.

The end view shows that at a shell thickness of 0.06 inches there is some damage to the front and back of the cylinder but most of the damage occurs to the top and bottom of the cylinder. For a stiffener spacing of 12.0 inches and a shell thickness of 0.12 inches there is still significant damage to the cylinder at the top and bottom but there is additional damage to the front and back of the cylinder. Finally at a stiffener spacing of 12.0 inches and a shell thickness of 0.24 inches most of the damage to the cylinder is at the back with some damage to the front and relatively little damage to the top and bottom. Reducing the stiffener spacing also effects the damage pattern by causing more damage to the front of the cylinder and less to the top and bottom of the cylinder than for the 12.0 inch stiffener spacing.

The resulting damage patterns for a perfect cylinder 12.0 inches in diameter (shell thickness to radius ratios from 0.01 to 0.04 and stiffener spacing to radius ratios from 1.0 to 2.0) are shown in Figures 29 and 30. The shock pressure for the 0.06 inch shell thickness is 500 psi for 1 ms, for the 0.12 inch shell thickness the pressure is 1000 psi for 1 ms and for the 0.24 inch shell thickness the pressure is 1900 psi for 1 ms.

At a shell thickness of 0.06 inches the pinching of the shell occurs for stiffener spacing of 12.0. 8.0 and 6.0 inches. At a stiffener spacing of 12.0 inches increasing the shell thickness causes the pinching of the shell to decrease until it is eliminated for the shell thickness of 0.24 inches. At stiffener spacing of less than 12.0 inches increasing the shell thickness causes the pinching of the shell to disappear for both the 0.12 and 0.24 inch shell thickness.

The end view shown that, for shell thickness of 0.06 and 0.12 inches, at a diameter of 12.0 inches there is a protrusion of the shell toward the shock wave approach direction. Increasing the shell thickness to 0.24 inches, for the three stiffener spacing investigated, causes the protrusion to be eliminated. Decreasing the stiffener spacing causes a decrease in damage to the cylinder and some

minor shifting of the damage pattern but the basic shape of the damages pattern remains constant.

The resulting damage for a perfect cylinder 18.0 inches in diameter (shell thickness to radius ratios from 0.0067 to 0.0267 and stiffener spacing to radius ratios from 0.67 to 1.33) is shown in Figures 31 and 32. The shock pressure for the 0.06 inch shell thickness is 500 psi for 1 ms, for the 0.12 inch shell thickness the pressure is 1000 psi for 1 ms and for the 0.24 inch shell thickness the pressure is 1700 psi for 1 ms.

In all cases, for the 18.0 inch diameter perfect cylinder there was no pinching of the shell near the stiffener. This cylinder is structurally much less stiff than the smaller diameter cylinders thus allowing the shell to collapse more readily without pinching near the stiffener.

From the end view it can be seen that the protrusion of the shell toward the explosion source occurs in all cases. For the thicker shell this protrusion is not as sharp as for the thinner shell. Decreasing the stiffener spacing does not greatly affect the damage patterns but does cause the damage levels to decrease.

The damage pattern for a 12.0 inch diameter cylinder, with a mode 6 initial imperfection, an amplitude of 5% of the shell thickness and no phase shift, is shown in Figures

33 and 34. The shock wave pressure varies from 500 psi for 1 ms for the 0.06 inch shell thickness to 1000 psi for 1 ms for the 0.12 inch shell thickness and finally to 1900 psi for 1 ms for the 0.24 inch shell thickness. These shock wave pressure are the same as for the perfect cylinder cases at a cylinder diameter of 12.0 inches.

The front view shows the pinching of the shell near the stiffener only occurs for the 0.06 inch shell thickness. For thicker shells the pinching is eliminated. The end views show that the initial mode 6 imperfection is seen in the final deformation pattern of the shell of the cylinder in all cases. Changing the shell thickness and the stiffener spacing has very little effect on the damage pattern. The damage level is reduced as the stiffener spacing is reduced and this is expected as the cylinder becomes stiffer with decreasing stiffener spacing.

The damage to an 8.0 inch cylinder, with initial imperfections consisting of the first 10 mode shapes with an amplitude of 1% of the shell thickness and with random phase shifts of the modes is shown in Figures 35 and 36. In these cases, the shock wave pressures had to be reduced from the pressures used in the perfect cylinders at the same diameter, because the cylinders completely collapsed at the pressures used in the perfect cylinder cases. The shock wave pressures were 500 psi for 1 ms for the 0.06 inch shell

thickness, 1000 psi for 1 ms for the 0.12 inch shell thickness and 2250 psi for 1 ms for the 0.24 inch shell thickness. At this diameter the cylinder was weakened to a greater extent, than for the larger diameter cases, by the initial imperfections introduced into the shell geometry.

The front view of the cylinder shows that there is very little pinching of the shell of the cylinder near the stiffeners. The end view shows the damage is much more localized to a smaller portion of the shell than for the larger diameter cylinders. The damage pattern is fairly consistent with only changes in the magnitude of the damage among the cases studied. In addition the initial imperfection pattern is still seen in the final damage pattern but the match is much less pronounced than for the later cases studied.

For a cylinder diameter of 12.0 inches with initial imperfections consisting of the first 10 modes shapes with an amplitude of 1% of the shell thickness with random phase shifts of the modes, the damage patterns are much more consistent. Figures 37 and 38 shown the resulting damage patterns. At this diameter the shock wave pressure is the same as for the perfect cylinder cases at the same diameter with pressures of 500 psi for 1 ms for the 0.06 inch shell thickness, 1000 psi for 1 ms for the 0.12 inch shell

thickness and 1900 psi for 1 ms for the 0.24 inch shell thickness.

The front view shows a similar damage pattern for all cases. The shell very distinctly dishes between the stiffeners in a manner similar to that seen in many underwater shock test cylinders. Changing the shell thickness and the stiffener spacing has very little effect on the damage pattern as seen from the front of the cylinder. The end view shows again that in all cases shown the damage pattern remains very consistent and only the damage levels change with changes in the stiffener spacing. The 0.24 inch shell thickness does show some shifting of the damage pattern but the same basic pattern is still evident.
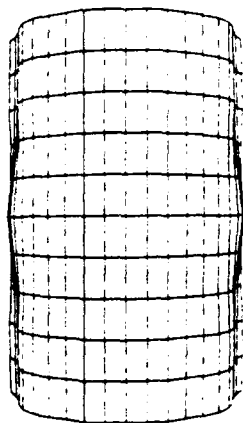
Finally, Figures 39 and 40 show the deformation of an 18.0 inch diameter cylinder with initial imperfections consisting of the first 10 mode shapes, each with an amplitude of 1% of the shell thickness with random phase shift. Again, the shock wave pressure was the same as for the perfect cylinder cases with a pressure of 500 psi for 1 ms for the 0.06 inch shell thickness, 1000 psi for 1 ms for the 0.12 inch shell thickness and 1700 psi for 1 ms for the 0.24 inch shell thickness.

From the front view it can be seen that the shell of the cylinder has deformed by dishing between the stiffeners in all cases. Decreasing the stiffener spacing reduced the
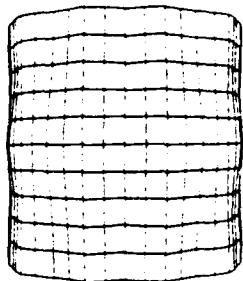
magnitude of the deformation but did not change the shape of the deformation. Increasing the shell thickness had little effect on the deformation pattern. The end views of the cylinder all show the same basic deformation pattern. Increasing the shell thickness had some effect on the damage pattern but the same deformation pattern is present in all the deformed cylinders.

Figure 27. Deformation of Three Dimensional Infinite Cylinder @ 5.0 ms, Front View, Perfect Cylinder, Dia.=8.0 in

Stiffener→
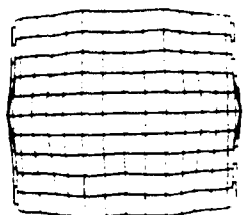Spacing
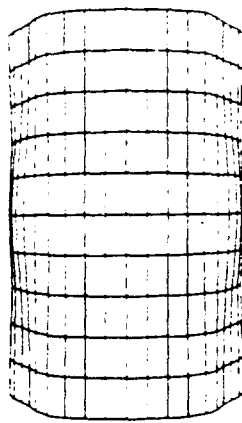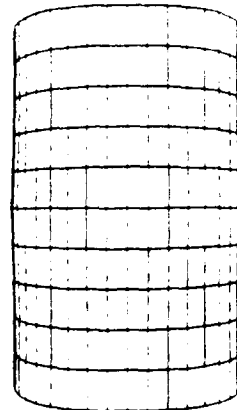Shell
Thickness
↓
0.06 in.
(600 psi
for 1 ms)

6.0 in.

8.0 in.

12.0 in.

0.12 in.
(1200 psi
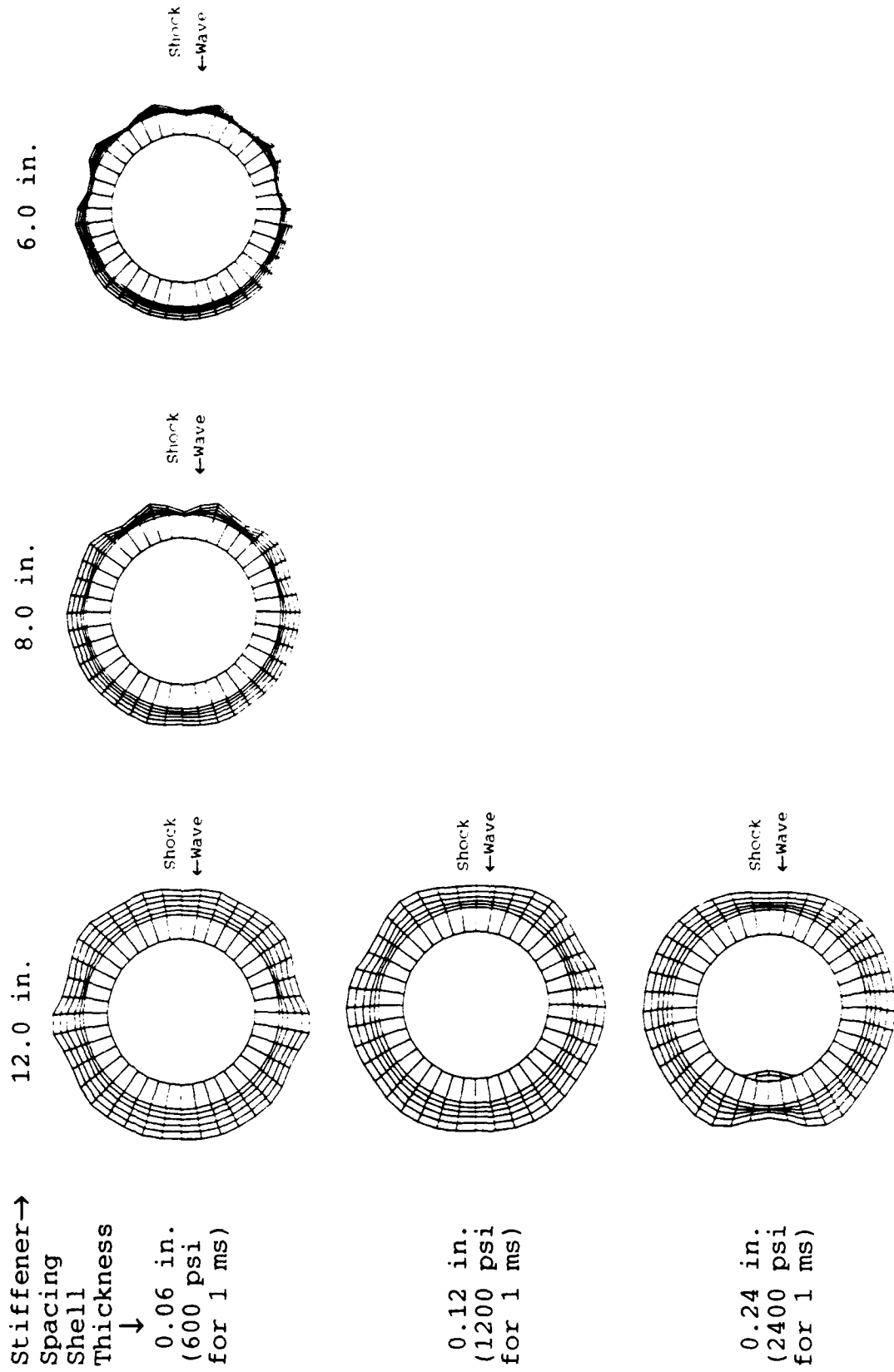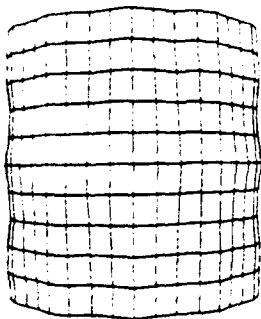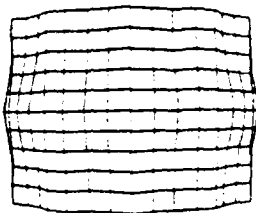for 1 ms)

0.24 in.
(2400 psi
for 1 ms)

Figure 28. Deformation of Three Dimensional Infinite Cylinder @ 5.0 ms, End View, Perfect Cylinder, Dia.=8.0 in

Stiffener→
Spacing
Shell
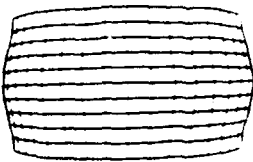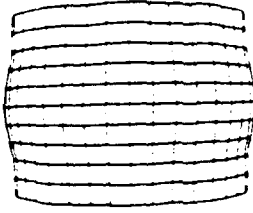Thickness
→ 0.06 in.
(500 psi
for 1 ms)

12.0 in.

8.0 in.

6.0 in.

0.12 in.
(1000 psi
for 1 ms)

0.24 in.
(1900 psi
for 1 ms)

Figure 29. Deformation of Three Dimensional Infinite Cylinder @ 5.0 ms, Front View, Perfect Cylinder, Dia.=12.0 in

39

Figure 30. Deformation of Three Dimensional Infinite Cylinder @ 5.0 ms, End View, Perfect Cylinder, Dia.=12.0 in

40

6.0 in.

8.0 in.

Stiffener→
Spacing
Shell
Thickness
→

12.0 in.

0.06 in.
(500 psi
for 1 ms)
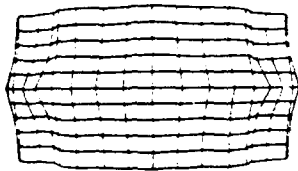
0.12 in.
(1000 psi
for 1 ms)

0.24 in.
(1700 psi
for 1 ms)

Figure 31. Deformation of Three Dimensional Infinite Cylinder @ 5.0 ms, Front View, Perfect Cylinder, Dia.=18.0 in

6.0 in.

8.0 in.

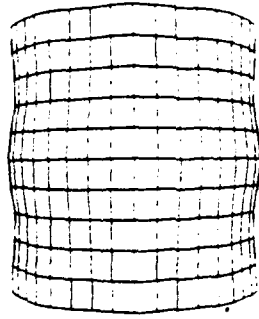12.0 in.

Stiffener→
Spacing
Shell
Thickness
→

0.06 in.
(500 psi
for 1 ms)

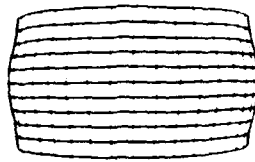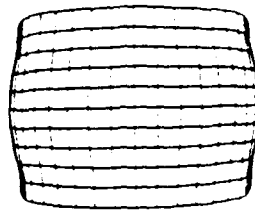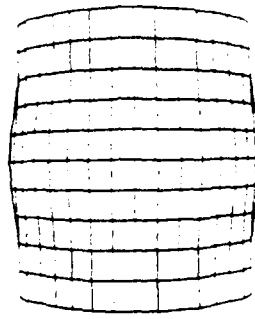0.12 in.
(1000 psi
for 1 ms)

0.24 in.
(1700 psi
for 1 ms)

Figure 32. Deformation of Three Dimensional Infinite Cylinder @ 5.0 ms, End View,
Perfect Cylinder, Dia.=18.0 in

42

Figure 33. Deformation of Three Dimensional Infinite Cylinder @ 5.0 ms, Front View, Mode 6 Initial Imperfection $A_6 = 0.05h$ no phase shift, Dia.=12.0 in
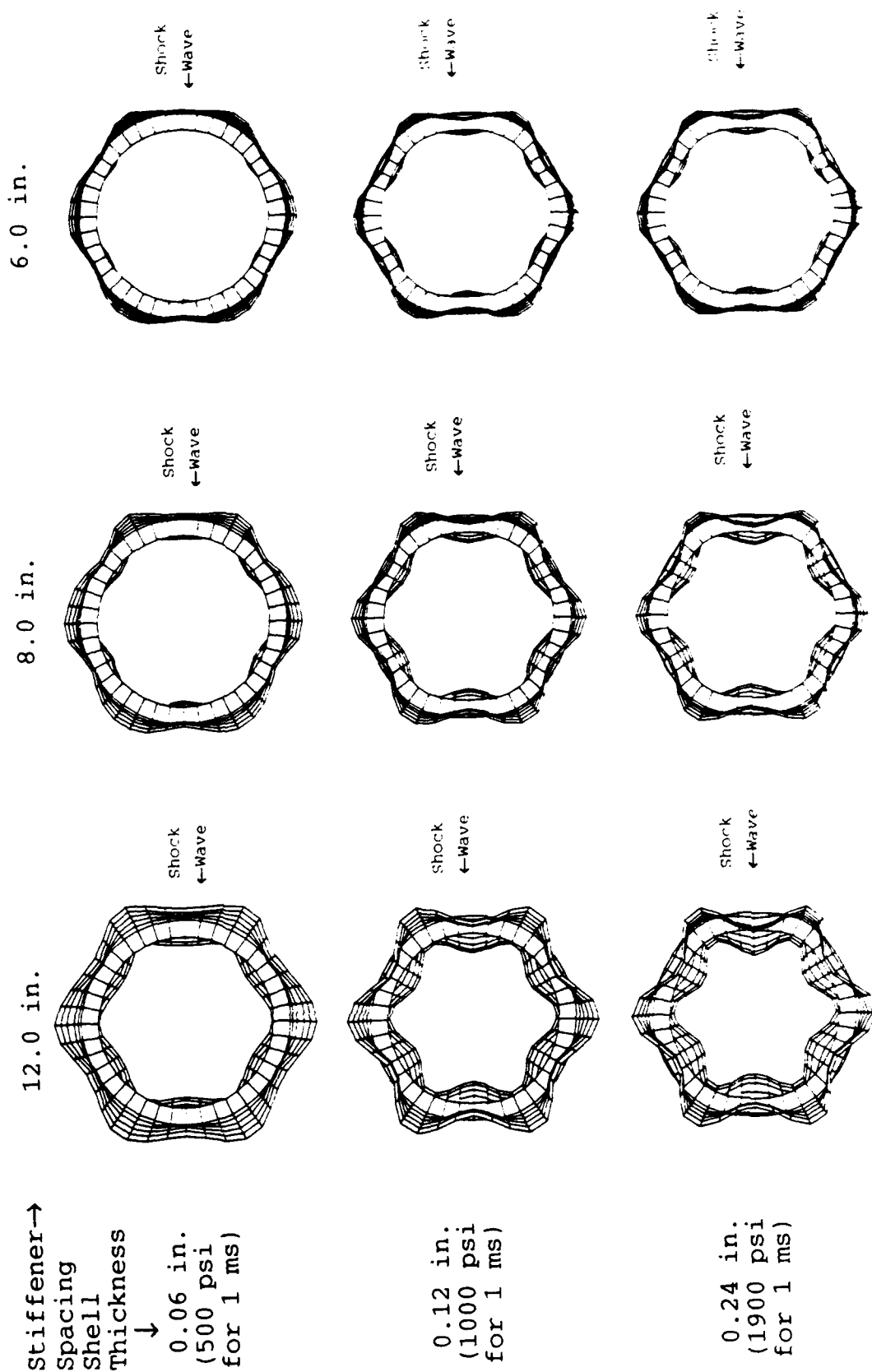
Figure 34. Deformation of Three Dimensional Infinite Cylinder @ 5.0 ms, End View, Mode 6 Initial Imperfection $A_6 = 0.05h$ no phase shift, Dia.=12.0 in
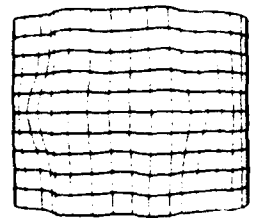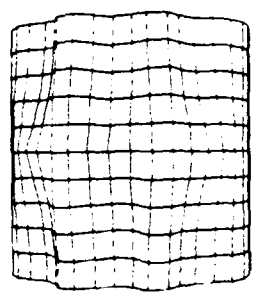
6.0 in.

8.0 in.
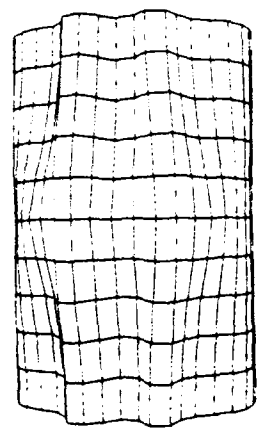
Stiffener→
Spacing
Shell
Thickness
↓
12.0 in.

0.06 in.
(500 psi
for 1 ms)

0.12 in.
(1000 psi
for 1 ms)
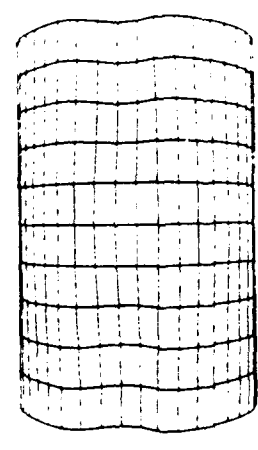
0.24 in.
(2250 psi
for 1 ms)
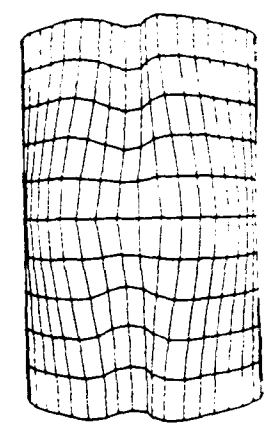
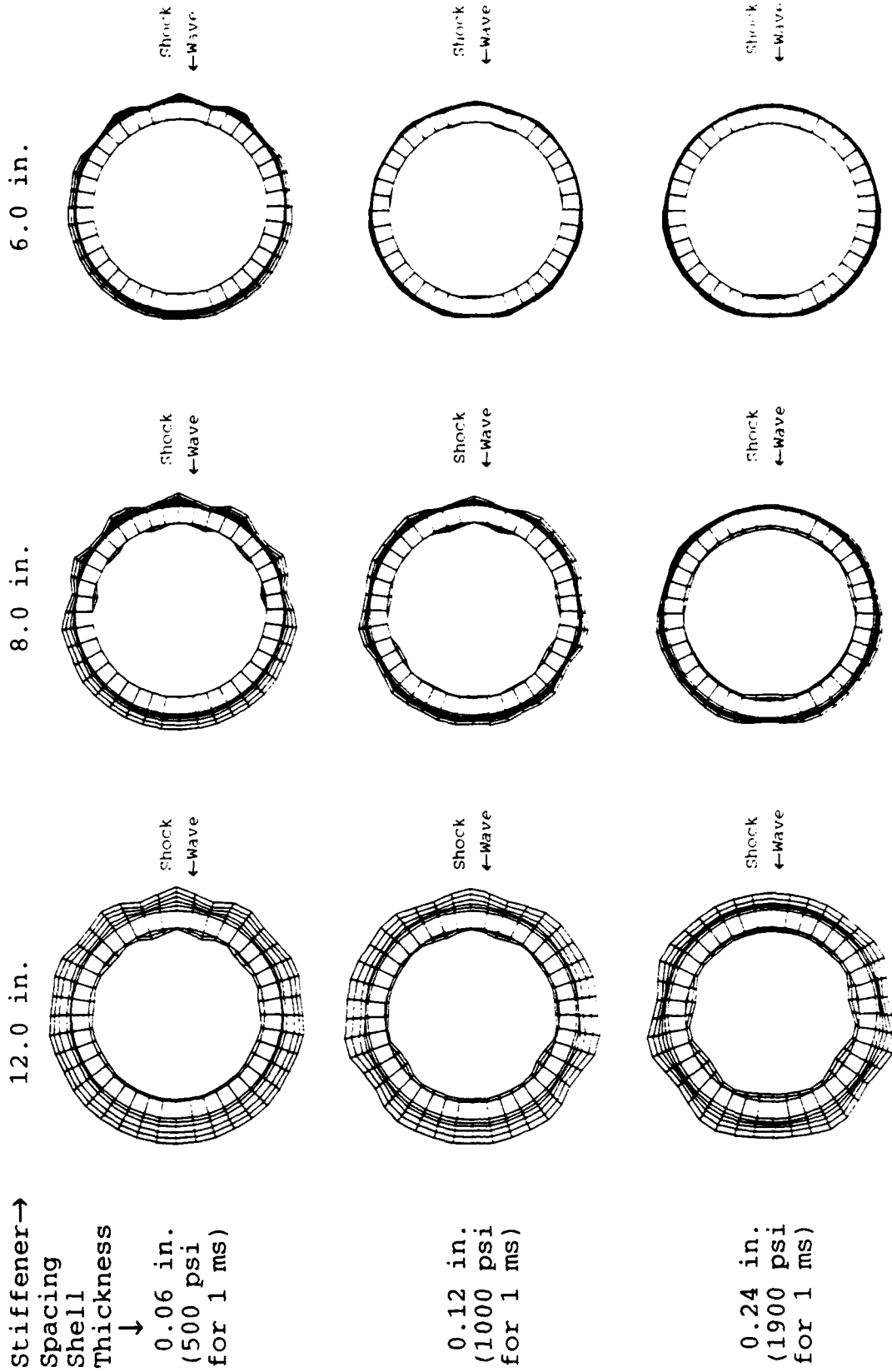Figure 35. Deformation of Three Dimensional Infinite Cylinder @ 5.0 ms, Front View, First 10 Modes Initial Imperfection $A_n = 0.01h$ with Random Phase Shift Dia.=8.0 in
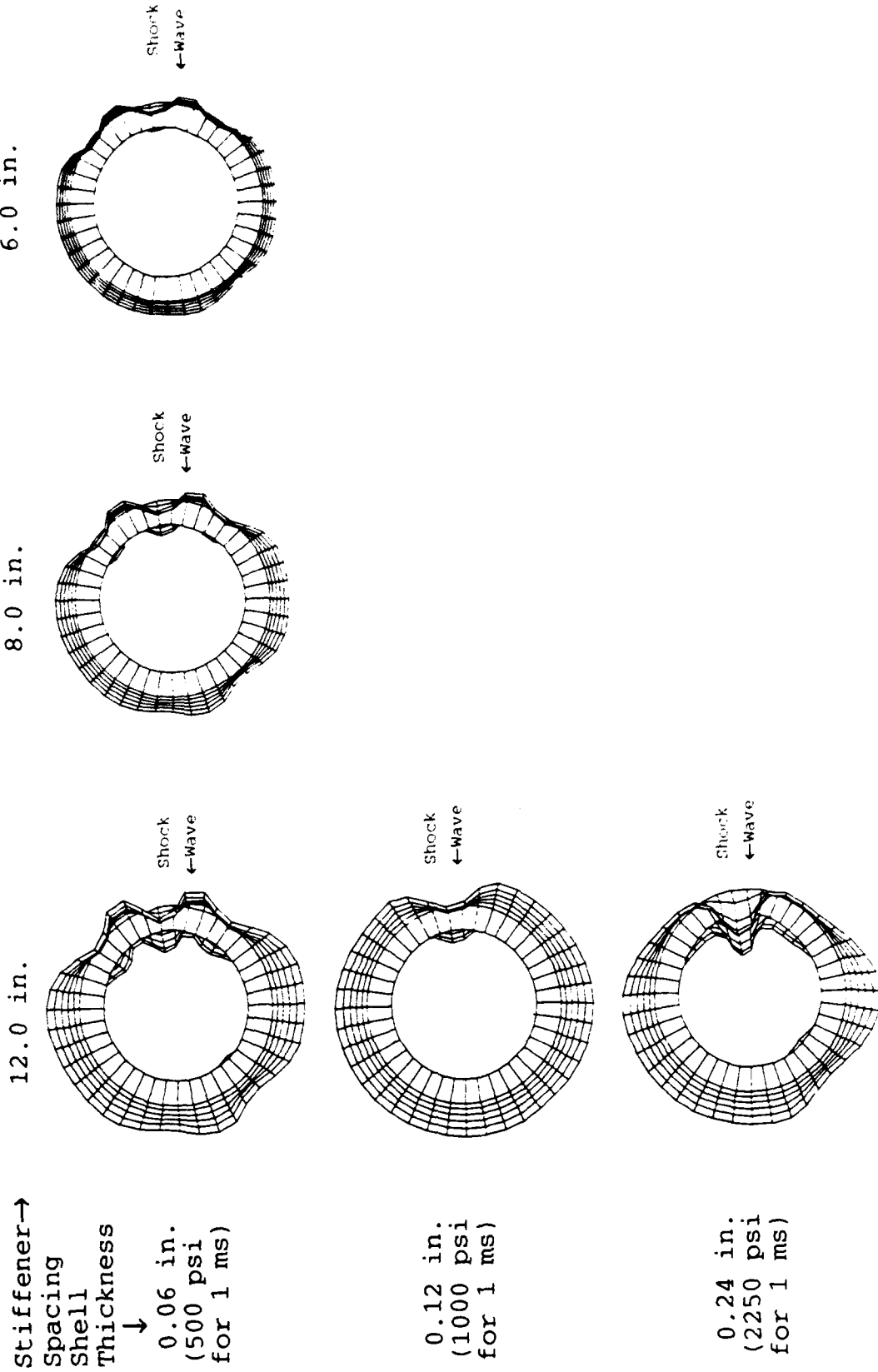
Figure 36. Deformation of Three Dimensional Infinite Cylinder @ 5.0 ms, End View, First 10 Modes Initial Imperfection $A_n = 0.01h$ with Random Phase Shift, Dia.=8.0 in

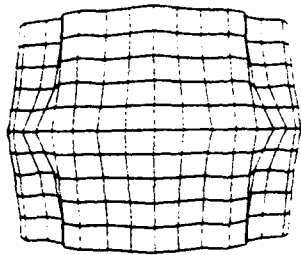Figure 37. Deformation of Three Dimensional Infinite Cylinder @ 5.0 ms, Front View, First 10 Modes Initial Imperfection $A_n = 0.01h$ with Random Phase Shift, Dia.=12.0 in

6.0 in.

8.0 in.

12.0 in.

Stiffener→
Spacing
Shell
Thickness
→

0.06 in.
(500 psi
for 1 ms)
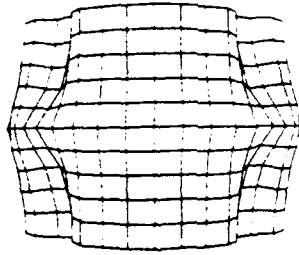
0.12 in.
(1000 psi
for 1 ms)

0.24 in.
(1900 psi
for 1 ms)

47

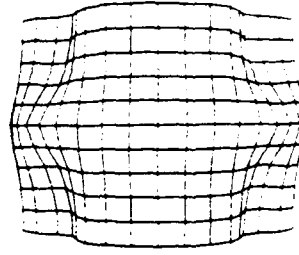Figure 38. Deformation of Three Dimensional Infinite Cylinder @ 5.0 ms, End View, First 10 Modes Initial Imperfection $A_n = 0.01h$ with Random Phase Shift, Dia.=12.0 in
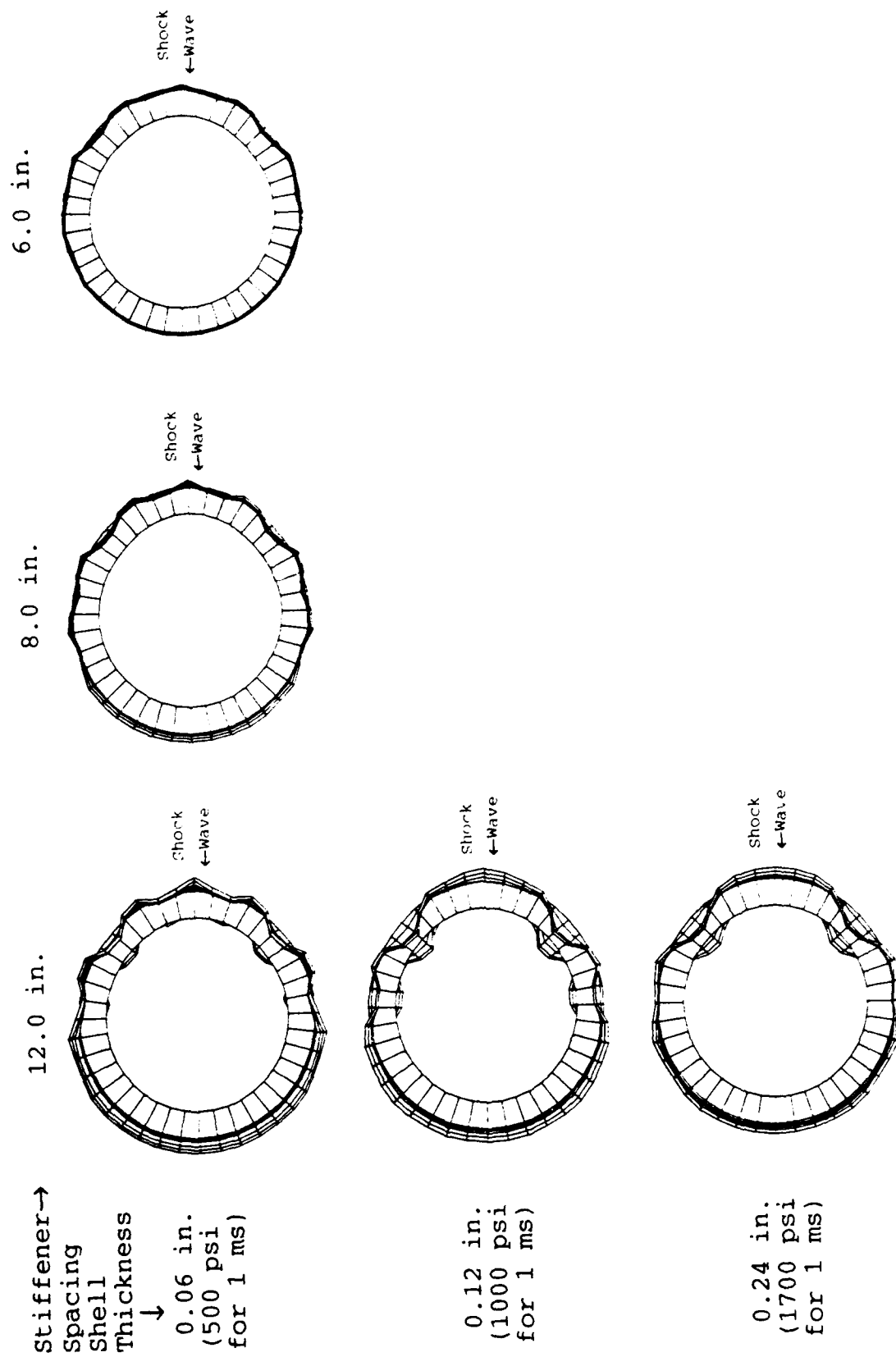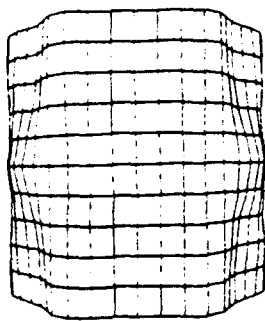
48
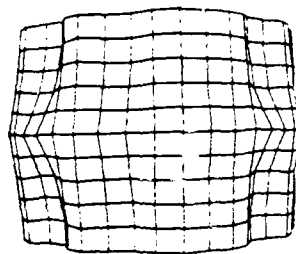
Figure 39. Deformation of Three Dimensional Infinite Cylinder @ 5.0 ms, Front View, First 10 Modes Initial Imperfection $A_n = 0.01h$ with Random Phase Shift, Dia.=18.0 in

49

Figure 40. Deformation of Three Dimensional Infinite Cylinder @ 5.0 ms, End View, First 10 Modes Initial Imperfection $A_n = 0.01h$ with Random Phase Shift, Dia.=18.0 in

V. THREE DIMENSIONAL RING STIFFENED FINITE LENGTH CYLINDER

From the three-dimensional infinite cylinder a three dimensional finite length cylinder was developed as shown in Figure 41. This cylinder is three feet long, 1 foot in diameter with two stiffeners evenly spaced 12 inches apart. The shell of the cylinder is mild steel 0.06 inches thick. The stiffeners are mild steel 0.12 inches thick and 1 inch deep. The endplate is HY-100 steel 0.25 inches thick. The HY-100 steel is modeled as an elastic-plastic material with a Young's modulus of 2.9×10^7 psi, a Poisson's ratio of 0.3, a hardening modulus of 5020 psi and a yield stress of 108,000 psi. This cylinder is modeled as a half cylinder with a plane of symmetry perpendicular to the axis of rotation. The model has 40 elements in the circumferential direction and 15 elements in the axial direction for a total of 600 elements and 921 nodes. The use of a half symmetry model with a symmetric boundary condition results in a smaller number of elements and greater computational efficiency for the finite element analysis. For details of the model input parameters see Appendix E.
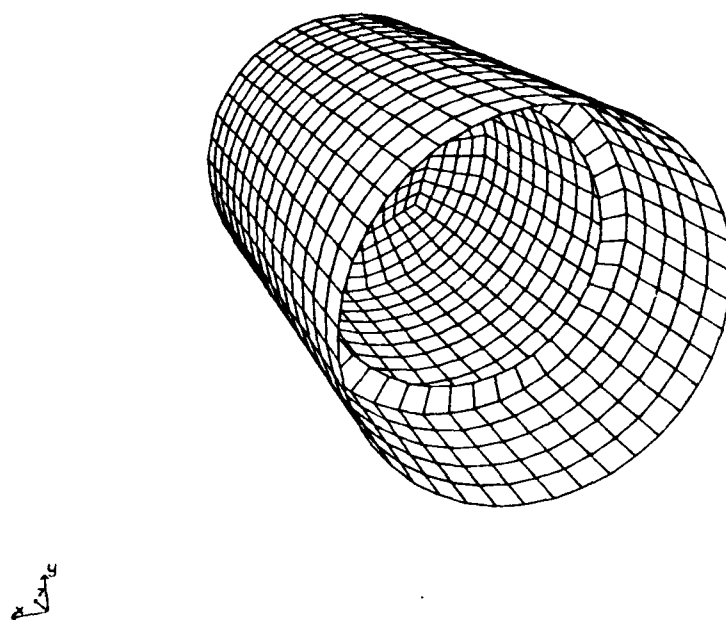
Figure 41.   Three Dimensional Ring Stiffened Finite Length
Cylinder Model

A. Perfect Cylinder Models

This cylinder was subjected to the same planar shock wave as in the previous models. The resulting damage pattern for a perfect cylinder can be seen in Figures 42 through 49. Again the side of the cylinder facing the planar shock wave shown a local raised area that was also seen in the previous models. In addition there is a pinch in the shell near the endplates and on either side of the stiffeners. This pinch was also noted by Chisum (1992) during his analysis of DNA models used for underwater shock testing. Most of the deformation of the cylinder shell occurs between 1.0 and 2.0 milliseconds (Figures 44 through 47). During the time from 1.0 to 2.0 milliseconds this kinetic energy is transferred to strain energy causing deformation of the shell. After 2.0 milliseconds the most of the plastic deformation has occurred and the cylinder shell then deforms only through elastic vibration (Figures 48 and 49). Figure 50 is a plot of the kinetic energy of the cylinder shell as a function of time. The shell has its maximum kinetic energy at 1 ms and then this energy rapidly decreases as it is dissipated into the surrounding medium and into the shell material as strain energy. Figure 51 shows the strain history of the element on the front of the cylinder exactly in the middle of the stiffeners. From this plot, at 1 millisecond the hoop strain is -5590 microstrain,
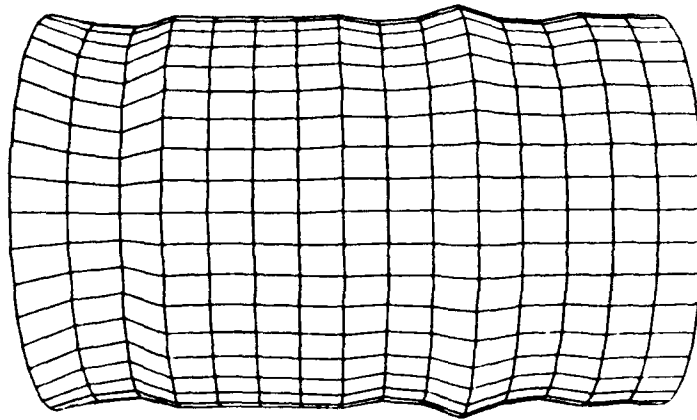
Front View @ 0.2 ms (deformations scaled up 50X)

Figure 42.   Deformation of Three Dimensional Ring Stiffened
Finite Length Cylinder Subjected to a Square Pressure Pulse
of 500 psi for 1 ms

Shock→
Wave
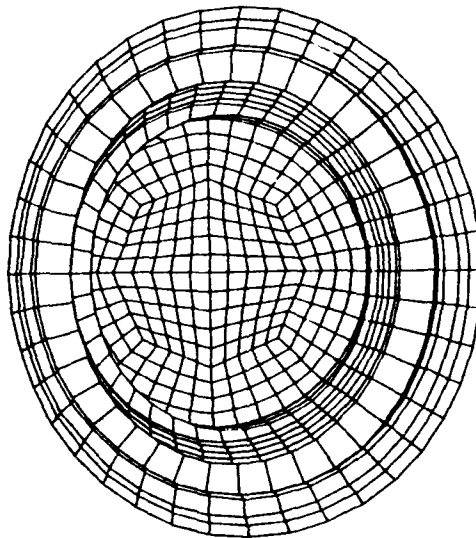
End View @ 0.2 ms (deformations scaled up 50X)

Figure 43.   Deformation of Three Dimensional Ring Stiffened
Finite Length Cylinder Subjected to a Square Pressure Pulse
of 500 psi for 1 ms

Front View @ 1.0 ms (deformations scaled up 2X)

Figure 44. Deformation of Three Dimensional Ring Stiffened
Finite Length Cylinder Subjected to a Square Pressure Pulse
of 500 psi for 1 ms

Shock→
Wave

End View @ 1.0 ms (deformations scaled up 2X)

Figure 45. Deformation of Three Dimensional Ring Stiffened
Finite Length Cylinder Subjected to a Square Pressure Pulse
of 500 psi for 1 ms

Front View @ 2.0 ms (deformations scaled up 2X)

Figure 46. Deformation of Three Dimensional Ring Stiffened
Finite Length Cylinder Subjected to a Square Pressure Pulse
of 500 psi for 1 ms

Shock→
Wave

End View @ 2.0 ms (deformations scaled up 2X)

Figure 47. Deformation of Three Dimensional Ring Stiffened
Finite Length Cylinder Subjected to a Square Pressure Pulse
of 500 psi for 1 ms

Front View @ 5.0 ms (deformations scaled up 2X)

Figure 48. Deformation of Three Dimensional Ring Stiffened
Finite Length Cylinder Subjected to a Square Pressure Pulse
of 500 psi for 1 ms

Shock→
Wave

End View @ 5.0 ms (deformations scaled up 2X)

Figure 49. Deformation of Three Dimensional Ring Stiffened
Finite Length Cylinder Subjected to a Square Pressure Pulse
of 500 psi for 1 ms
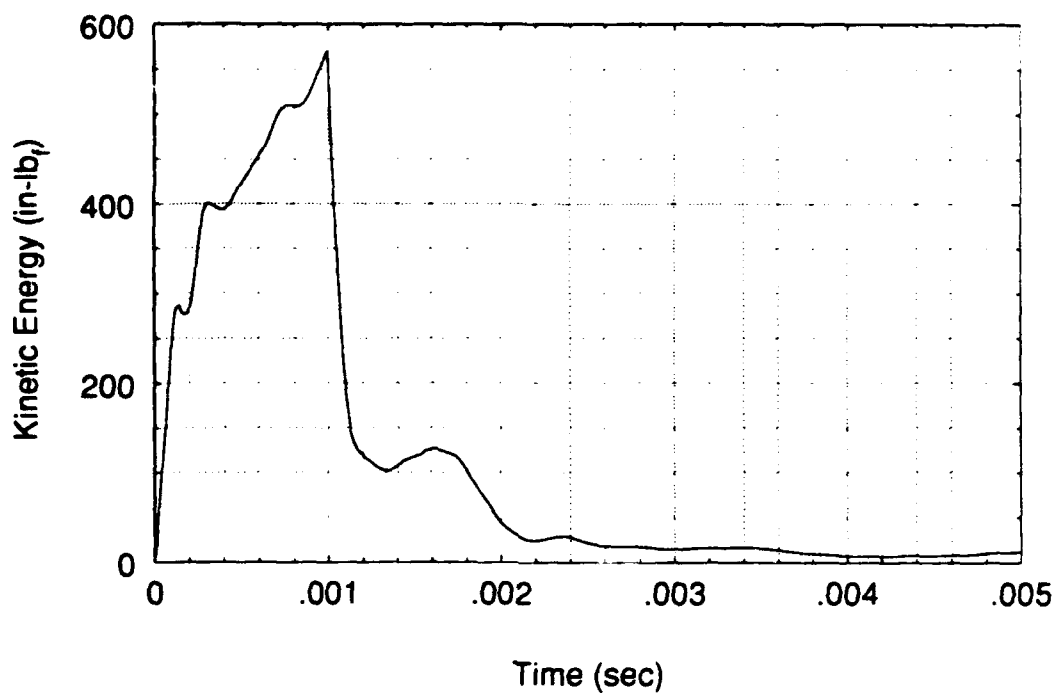
Figure 50.   Kinetic Energy of Shell Material
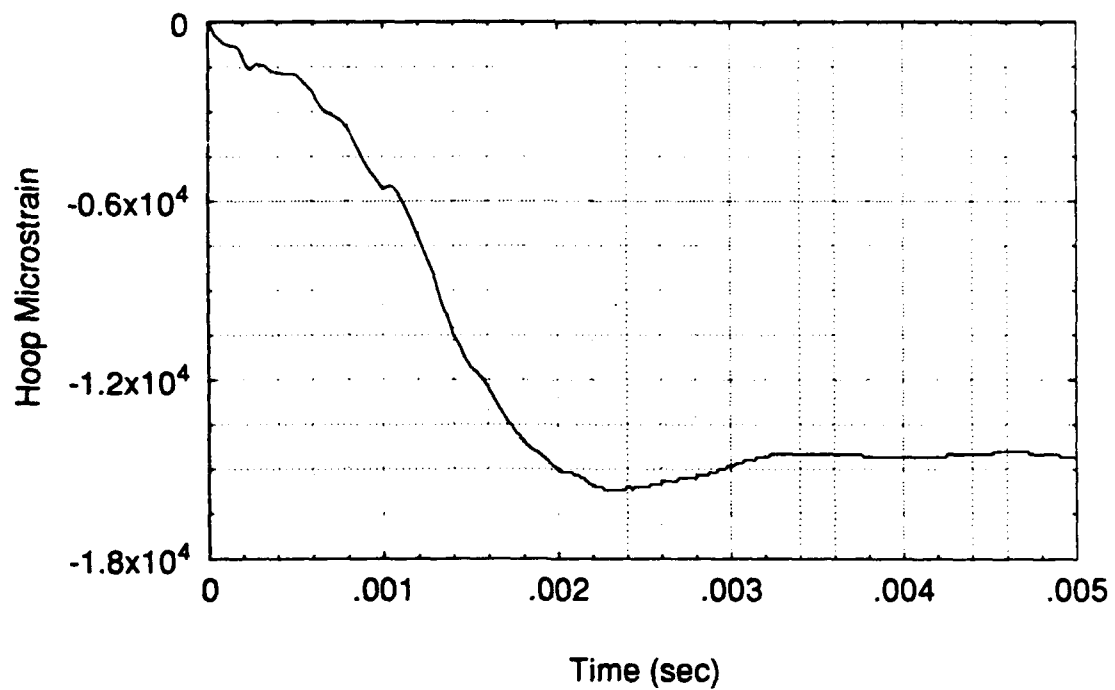
Figure 51.   Hoop Strain of Front Middle Element

at 2 milliseconds the hoop strain is -15000 microstrain and at 5 milliseconds the hoop strain is -14600 microstrain. The strain at 5 milliseconds is permanent plastic strain. Most of this plastic strain occurred between 1 and 2 milliseconds with very little additional strain occurring after 2 milliseconds. This confirms the previously noted timing of the deformation of the shell of the cylinder. Most of the damage to the shell occurs between 1 and 2 milliseconds.

B. Imperfect Cylinder Models

The addition of initial imperfections greatly changes the resulting deformation pattern of the shell of the cylinder. The addition of a mode 6 imperfection (shown in Figure 52) with a modal amplitude of 5% of the shell thickness and with no random phase shift results in the final damage pattern shown in Figure 53 and 54. The end view clearly shows the strong effect of the mode 6 initial imperfection causing the final deformation to follow this initial imperfection. The front view of the cylinder shows that the pinching of the shell near the endplates and stiffeners is very much reduced due to the introduction of this imperfection.

An investigation into the effect of the modal amplitude on the final deformation pattern showed that very small
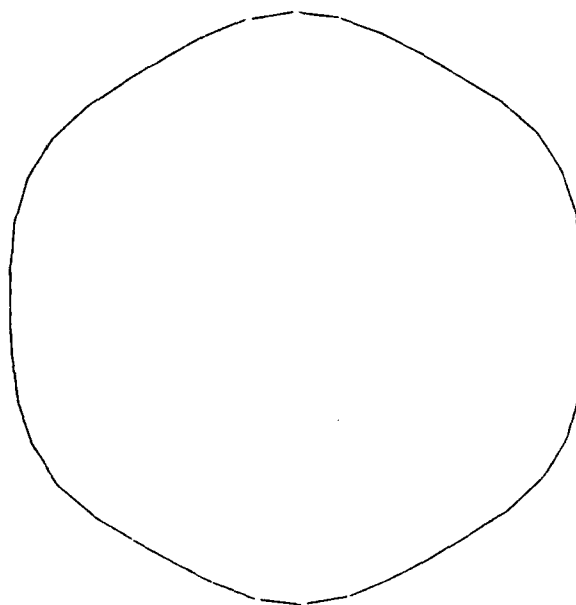
Initial Imperfection (imperfections scaled up 100X)

Figure 52.   Three Dimensional Ring Stiffened Finite Length
Cylinder Subjected to a Square Pressure Pulse of 500 psi for
1 ms, Mode 6 Initial Imperfection $A_6 = 0.05h$ no phase shift
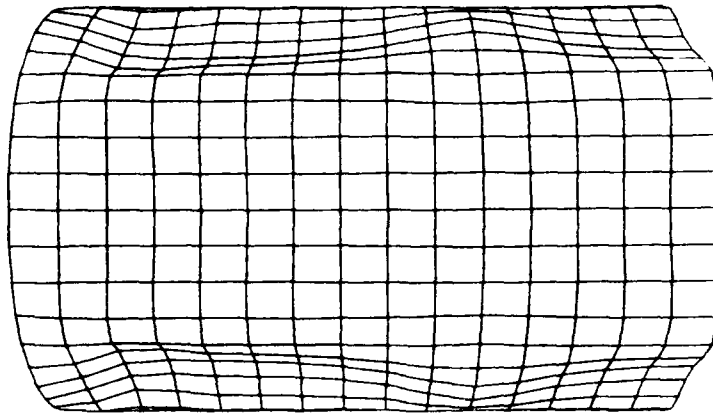
Front View @ 5.0 ms

Figure 53. Three Dimensional Ring Stiffened Finite Length Cylinder Subjected to a Square Pressure Pulse of 500 psi for 1 ms, Mode 6 Initial Imperfection $A_6 = 0.05h$ no phase shift

Shock→
Wave
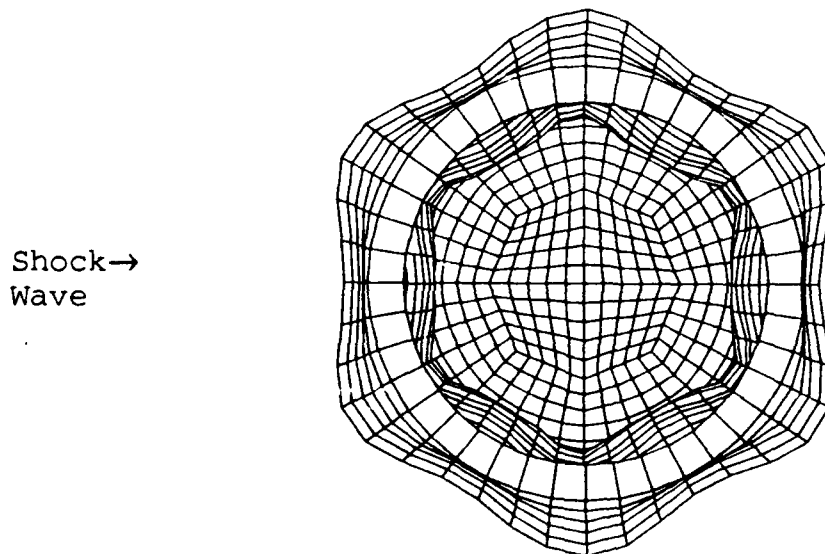
End View @ 5.0 ms

Figure 54. Three Dimensional Ring Stiffened Finite Length Cylinder Subjected to a Square Pressure Pulse of 500 psi for 1 ms, Mode 6 Initial Imperfection $A_6 = 0.05h$ no phase shift

modal amplitudes have a significant effect on the response of the cylinder. An initial imperfection consisting of the first 10 mode shapes with varying modal amplitudes and random phase shifts is shown in Figure 55. The shell deformation again follows the initial imperfections present in the shell structure. As the modal amplitudes increase the deformation of the shell of the cylinder also increases. At a modal amplitude of 0.01% of the shell thickness (Figures 56 and 57) the front of the cylinder is distinctly raised toward the explosive charge as in the perfect cylinder. But, it can also be seen from the end view that the deformation pattern even at this magnitude of imperfection has changed from the pattern for the perfect cylinder. At a model amplitude of 0.05% (Figures 58 and 59) this alteration of the pattern is quite obvious. The pinching of the shell of the cylinder persists until higher modal amplitudes are reached (Figures 60 through 63). Finally at a modal amplitude of 0.5% of the shell thickness (Figures 62 and 63) the pinching of the shell is eliminated. Increasing the amplitude further results in increased damage to the shell due to the shock wave (Figures 64 through 67). It should be noted that an amplitude of 0.5% of the shell thickness represents a modal amplitude of 0.0003 inches for this model. This magnitude of imperfections would almost certainly be present in a test cylinder.

Initial Imperfection (imperfections scaled up 200X)

Figure 55.   Three Dimensional Ring Stiffened Finite Length
Cylinder Subjected to a Square Pressure Pulse of 500 psi for
1 ms, First 10 Modes with Random Phase Shift

63

Front View @ 5.0 ms $A_n = 0.0001h$ with Random Phase Shift

Figure 56.   Deformation of Three Dimensional Ring Stiffened
Finite Length Cylinder Subjected to a Square Pressure Pulse
of 500 psi for 1 ms

Shock→
Wave
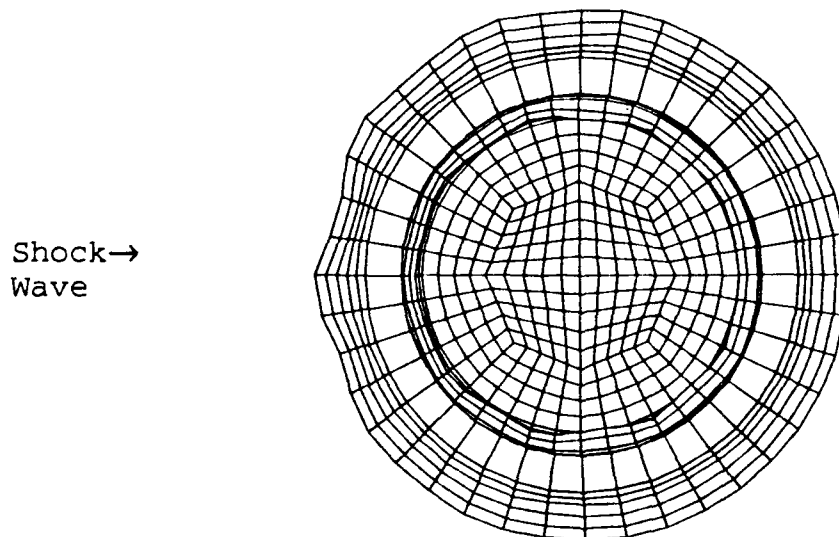
End View @ 5.0 ms $A_n = 0.0001h$ with Random Phase Shift

Figure 57.   Deformation of Three Dimensional Ring Stiffened
Finite Length Cylinder Subjected to a Square Pressure Pulse
of 500 psi for 1 ms
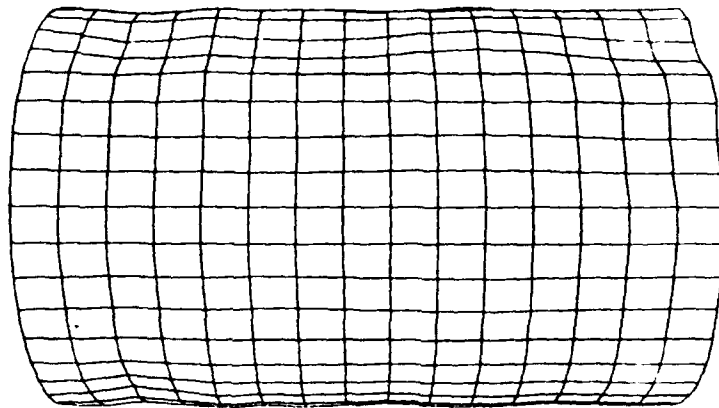
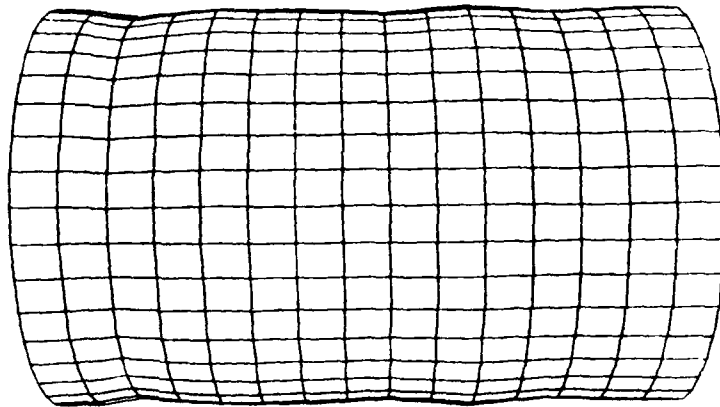Front View @ 5.0 ms $A_n = 0.0005h$ with Random Phase Shift

Figure 58.   Deformation of Three Dimensional Ring Stiffened
Finite Length Cylinder Subjected to a Square Pressure Pulse
of 500 psi for 1 ms

Shock→
Wave
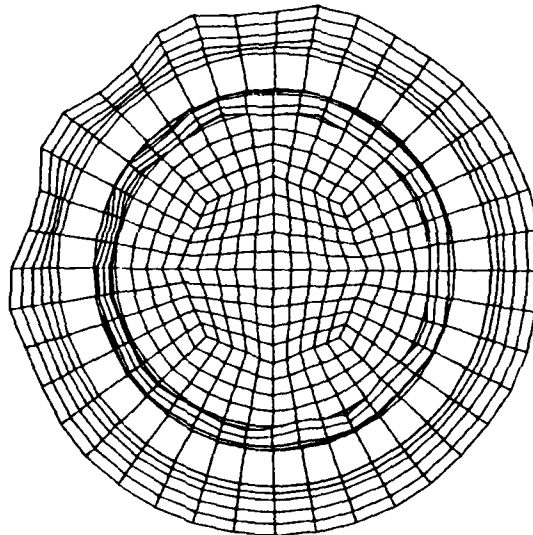
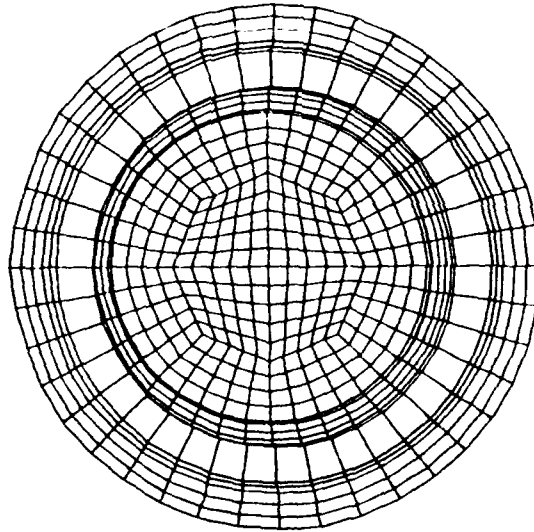End View @ 5.0 ms $A_n = 0.0005h$ with Random Phase Shift

Figure 59.   Deformation of Three Dimensional Ring Stiffened
Finite Length Cylinder Subjected to a Square Pressure Pulse
of 500 psi for 1 ms

65
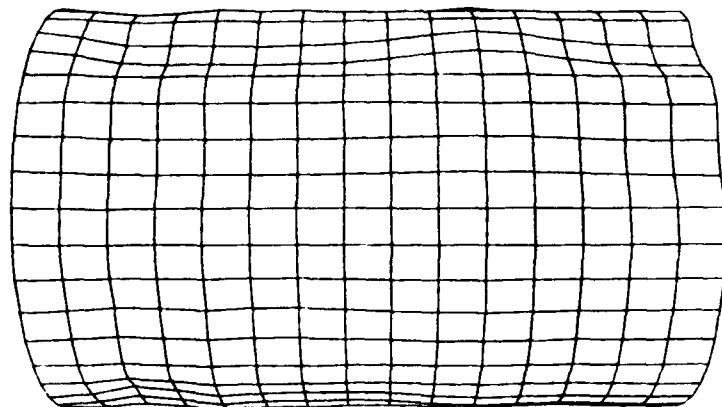
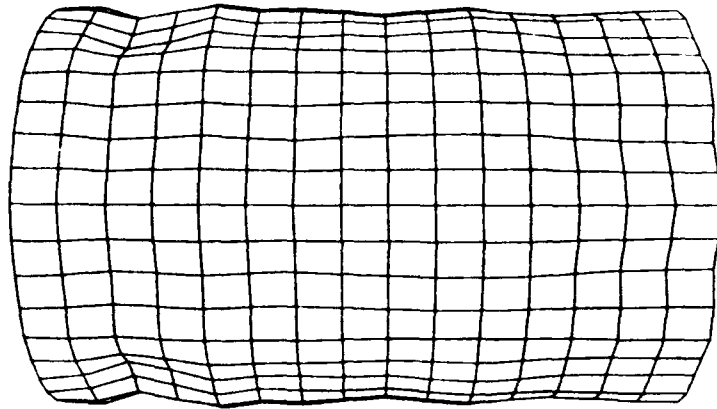Front View @ 5.0 ms $A_n = 0.001h$ with Random Phase Shift

Figure 60. Deformation of Three Dimensional Ring Stiffened
Finite Length Cylinder Subjected to a Square Pressure Pulse
of 500 psi for 1 ms

Shock→
Wave
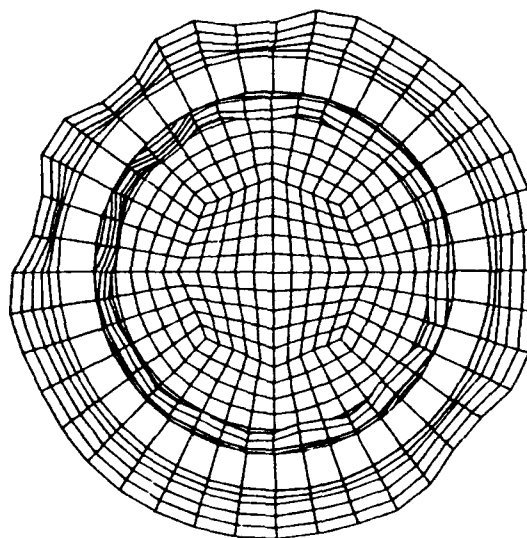
End View @ 5.0 ms $A_n = 0.001h$ with Random Phase Shift

Figure 61. Deformation of Three Dimensional Ring Stiffened
Finite Length Cylinder Subjected to a Square Pressure Pulse
of 500 psi for 1 ms
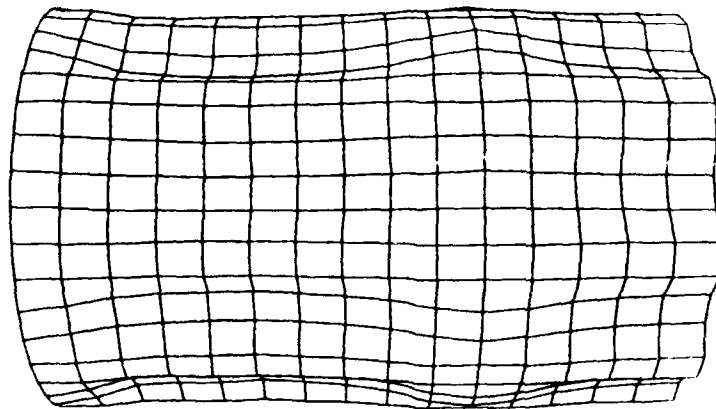
Front View @ 5.0 ms $A_n = 0.005h$ with Random Phase Shift

Figure 62. Deformation of Three Dimensional Ring Stiffened
Finite Length Cylinder Subjected to a Square Pressure Pulse
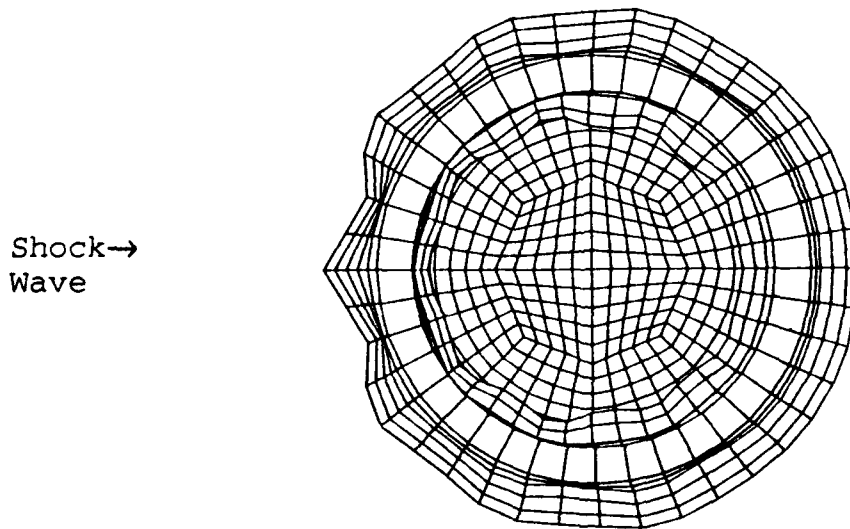of 500 psi for 1 ms

Shock→
Wave
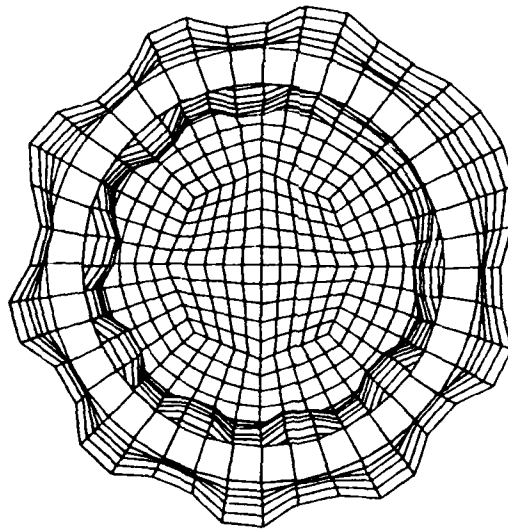
End View @ 5.0 ms $A_n = 0.005h$ with Random Phase Shift

Figure 63. Deformation of Three Dimensional Ring Stiffened
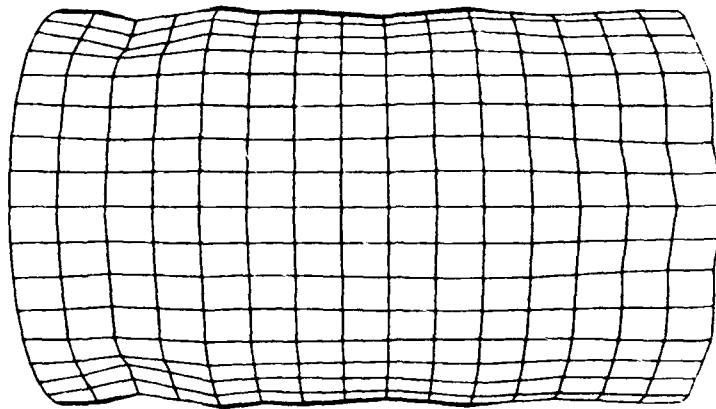Finite Length Cylinder Subjected to a Square Pressure Pulse
of 500 psi for 1 ms
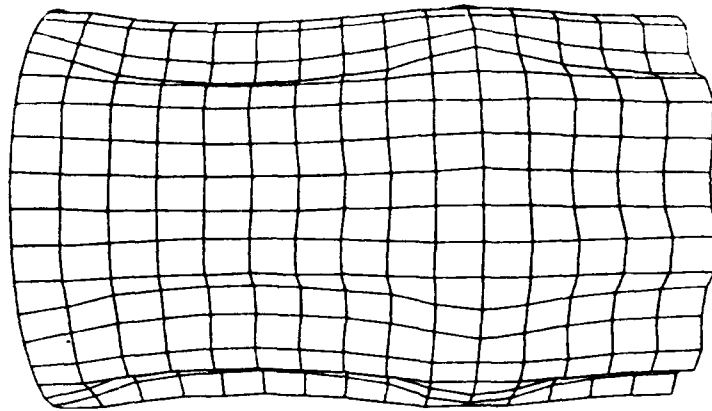
Front View @ 5.0 ms $A_n = 0.01h$ with Random Phase Shift

Figure 64.   Deformation of Three Dimensional Ring Stiffened
Finite Length Cylinder Subjected to a Square Pressure Pulse
of 500 psi for 1 ms

Shock→
Wave
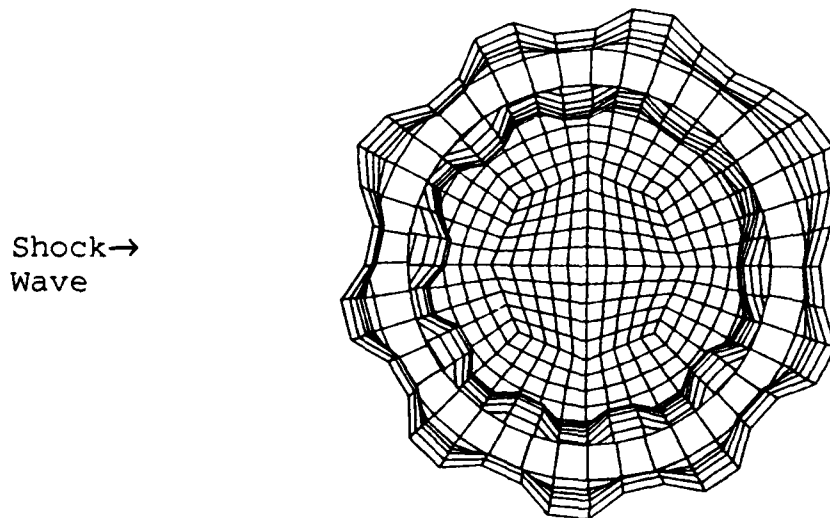
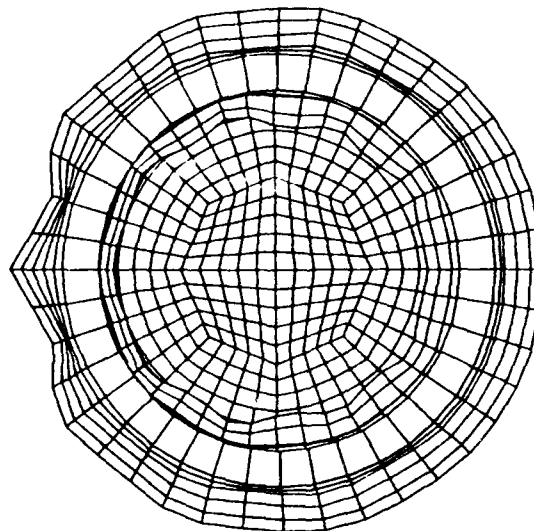End View @ 5.0 ms $A_n = 0.01h$ with Random Phase Shift

Figure 65.   Deformation of Three Dimensional Ring Stiffened
Finite Length Cylinder Subjected to a Square Pressure Pulse
of 500 psi for 1 ms
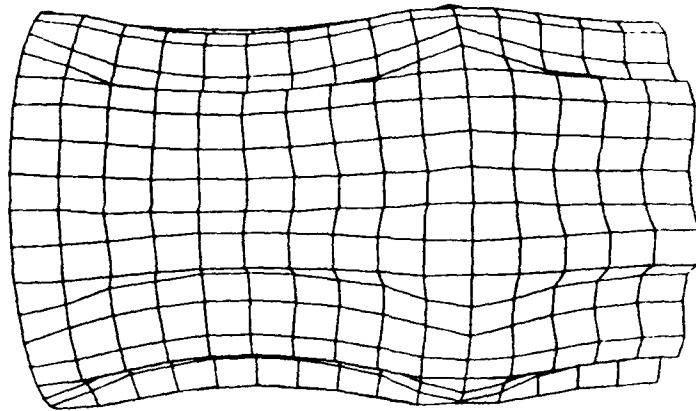
Front View @ 5.0 ms $A_n = 0.05h$ with Random Phase Shift

Figure 66.   Deformation of Three Dimensional Ring Stiffened
Finite Length Cylinder Subjected to a Square Pressure Pulse
of 500 psi for 1 ms

Shock→
Wave
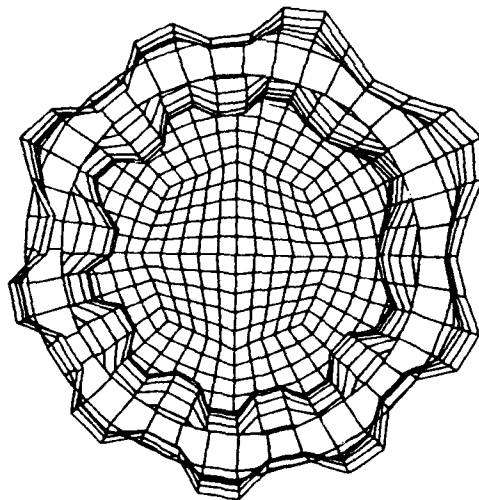
End View @ 5.0 ms $A_n = 0.05h$ with Random Phase Shift

Figure 67.   Deformation of Three Dimensional Ring Stiffened
Finite Length Cylinder Subjected to a Square Pressure Pulse
of 500 psi for 1 ms

69

The development of a raised section on the cylinder facing the shock wave was unexpected. With the previous perfect cylinder the shock wave impacted the cylinder along the line of nodes at the front of the cylinder. The cylinder was then rotated so that the shock wave would impact the cylinder along a line of elements. The resulting deformation pattern is shown in Figure 68. There is still a local raised section on the cylinder facing the shock wave direction. Thus, it is felt that the shot geometry of the finite element mesh is not a contributing factor to the development of this raised section.

In addition, a very specific imperfection was introduced in the five nodes facing the explosive charge centrally located in the midbay of the cylinder. This imperfection was an inward imperfection of the node locations with an amplitude of 1% of the shell thickness (0.006 inches). The damage pattern resulting from a 500 psi 1 millisecond shock wave is shown in Figure 69.

The use of Hughes-Liu shell element (Hughes 1981) vice the Belytschko-Tsay shell element was investigated. The Hughes-Liu shell element does not use many of the simplifying assumptions used in formulating the Belytschko-Tsay shell element. As a result, the use of the Hughes-Liu shell element requires longer computational times that may not be acceptable in certain models. Figures 70 and 71 show

70
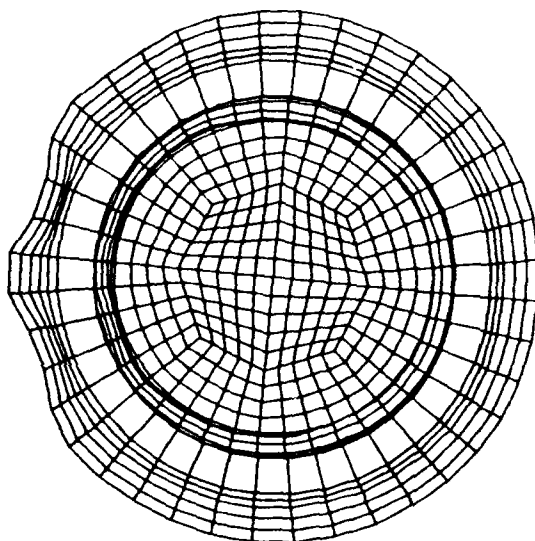
Shock→
Wave

End View @ 5.0 ms

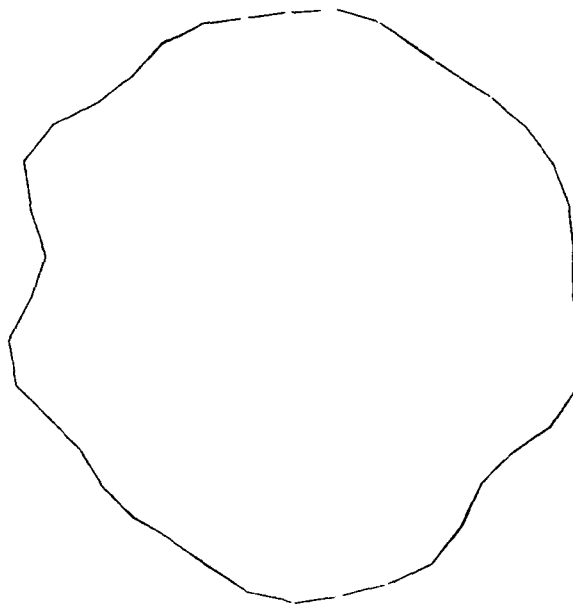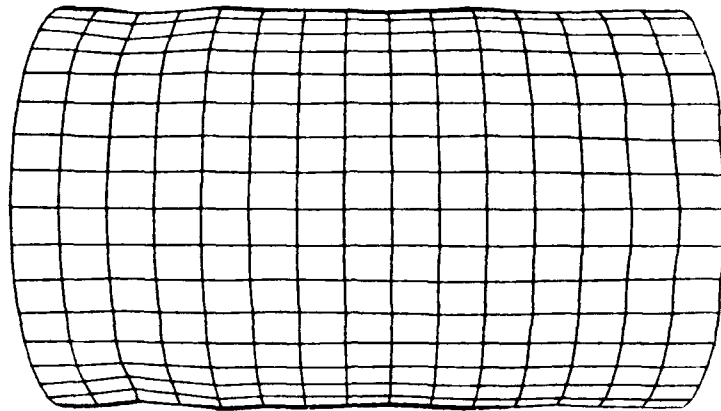Figure 68.   Deformation of Three Dimensional Ring Stiffened
Finite Length Cylinder Subjected to a Square Pressure Pulse
of 500 psi for 1 ms, Cylinder Rotated 4.5 Degrees

Shock→
Wave
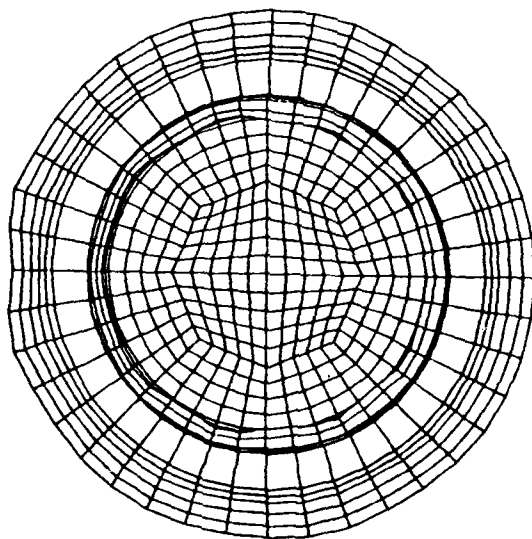
End View @ 5.0 ms

Figure 69.   Three Dimensional Finite Cylinder Subjected to a
Square Pressure Pulse of 500 psi 1 ms, Initial Imperfection
Front Midbay Nodes 1% Offset Radially Inward

the resulting deformation to a model using Hughes-Liu shell elements. This model is identical to the previous models with the exception of the use of the Hughes-Liu shell element. This model has initial imperfections with the first 1C modes and modal amplitudes of 1% of the shell thickness and random phase shifts. Comparison of Figures 70 and 71 with Figures 64 and 65 shows that the Hughes-Liu and the Belytschko-Tsay shell elements have the same final deformations. In this case the use of the numerically more complicated Hughes-Liu shell element is not warranted.

C. Exponential Decay Shock Wave

The use of an explosive shock wave modeled as a square wave is representative of a very large explosion at a great standoff distance from the cylinder. In order to model a smaller explosion close to the cylinder a pressure profile corresponding to that produced by 40 pounds of PETN at a standoff distance of 30 feet was used. The pressure time history of the resulting shock wave is shown in Figure 72. This explosion produces a peak pressure of 1839 psi and an exponentially decaying pressure history with a time constant of 0.311 milliseconds. The resulting damage to the cylinder from this shock wave is shown in Figure 73 through 75. From the offset view it can be seen that the response of the cylinder is different from that to the previous plane wave.
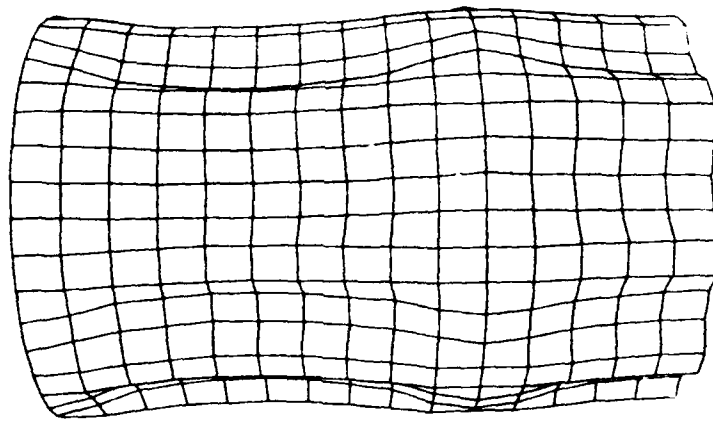
Front View @ 5.0 ms

Figure 70. Three Dimensional Ring Stiffened Finite Length
Cylinder Hughes-Liu Shell Elements Subjected to a Square
Pressure Pulse of 500 psi for 1 ms, Initial Imperfection
First 10 Modes $A_n=0.01h$ with Random Phase Shift

Shock$\rightarrow$
Wave
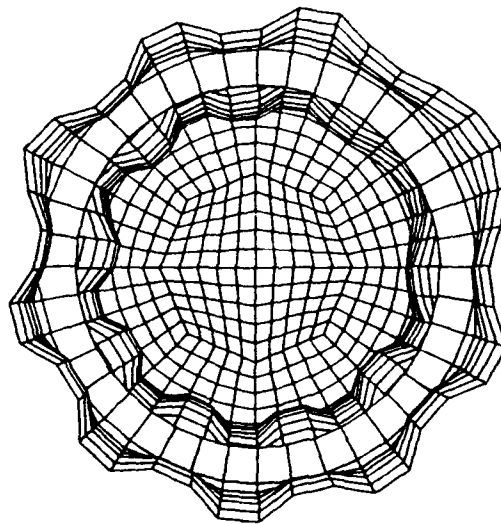
End View @ 5.0 ms

Figure 71. Three Dimensional Ring Stiffened Finite Length
Cylinder Hughes-Liu Shell Elements Subjected to a Square
Pressure Pulse of 500 psi for 1 ms, Initial Imperfection
First 10 Modes $A_n=0.01h$ with Random Phase Shift

73
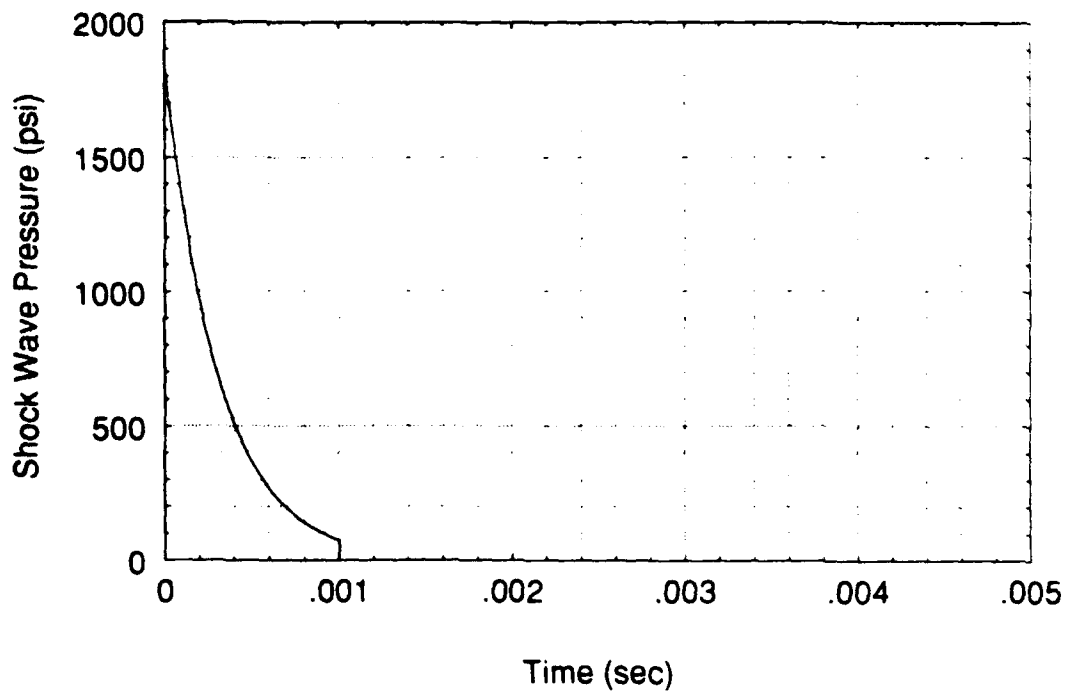
Figure 72. Pressure Time History of Shock Wave from 40 lbs
PETN with a 30 foot Standoff and 1 ms Surface Cutoff Time
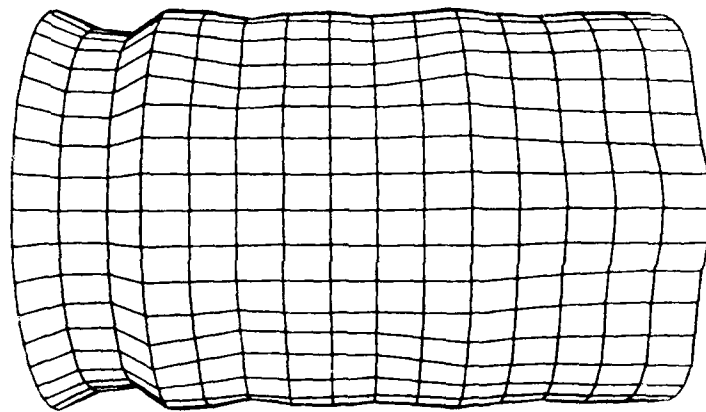
Front View @ 5.0 ms

Figure 73. Three Dimensional Ring Stiffened Finite Length
Cylinder Subjected to a Pressure Pulse from 40 lbs PETN 30
Foot Standoff
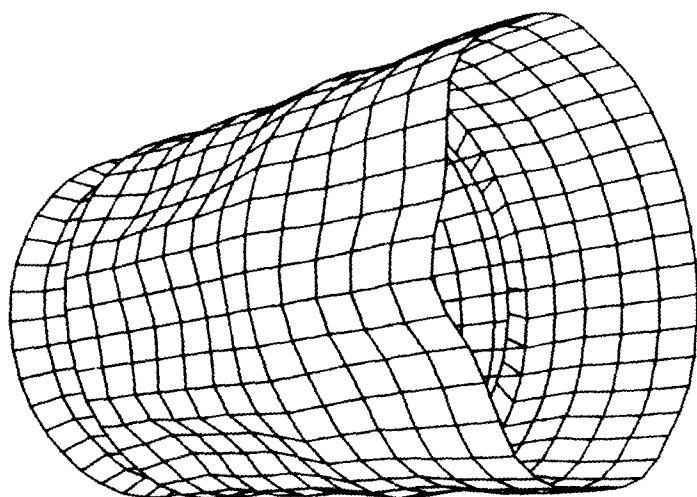
Offset View @ 5.0 ms

Figure 74.   Three Dimensional Ring Stiffened Finite Length
Cylinder Subjected to a Pressure Pulse from 40 lbs PETN 30
Foot Standoff
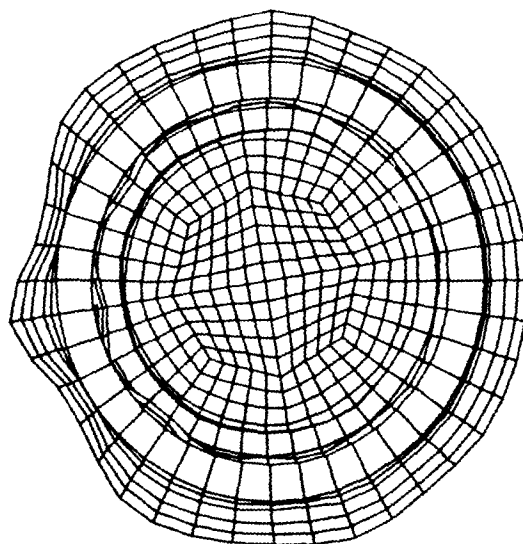
Shock→
Wave

End View @ 5.0 ms

Figure 75.   Three Dimensional Ring Stiffened Finite Length
Cylinder Subjected to a Pressure Pulse from 40 lbs PETN 30
Foot Standoff Final

75

The small standoff distance causes the shock wave to be a spherical wave at the cylinder. The midbay still has a protrusion of the shell material toward the explosive charge however the endbay shell material has a depression of the shell facing the charge. Also evident from the front view is the severe pinching of the shell near the endplate and on either side of the stiffener. This pinching was very severe near the endplate.

The introduction of a 5% mode 6 imperfection to the model (Figure 76) results in the deformations shown in Figure 77 and 78. Again, it is evident that the damage pattern of the cylinder due to the explosive shock clearly followed the initial imperfection. The pinching of the shell material near the endplate and stiffeners was reduced but not eliminated.

Introducing an imperfection of the first 10 mode shapes with a modal amplitude of 1% of the shell thickness with random phase shifts (Figure 79) results in the final damage pattern shown in Figures 80 and 81. The deformation of the shell of the cylinder was again influenced by the initial imperfection pattern. The local pinching of the shell material on either side of the stiffener was eliminated and the pinching near the endplate was reduced in magnitude.
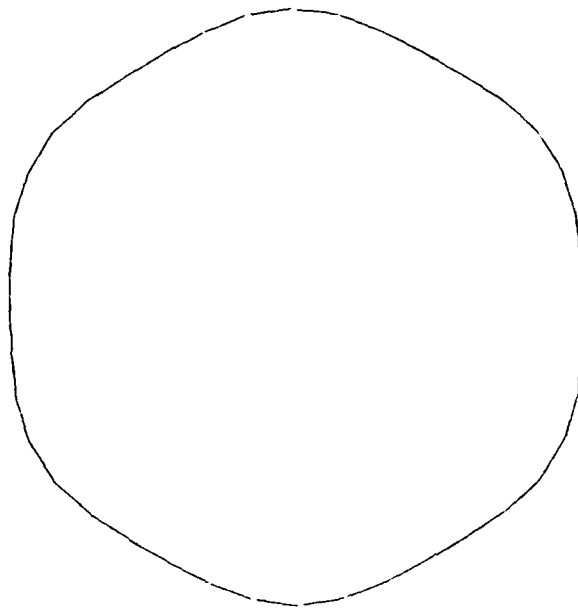
Initial Imperfection (imperfections scaled up 100X)

Figure 76. Three Dimensional Ring Stiffened Finite Length
Cylinder Subjected to a Pressure Pulse from 40 lbs PETN 30
Foot Standoff, Initial Mode 6 Imperfection $A_6 = 0.05h$ no phase
shift
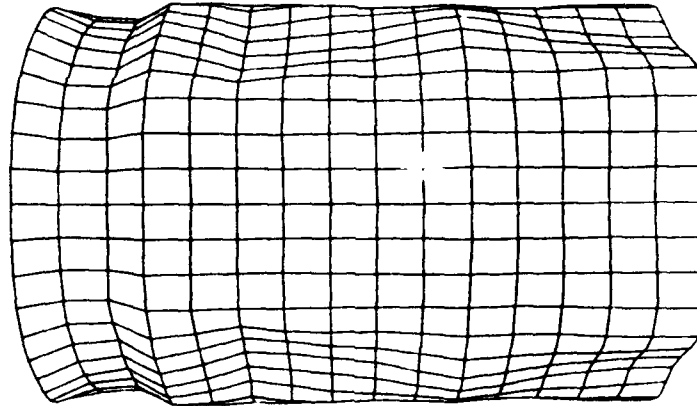
Front View @ 5.0 ms

Figure 77. Three Dimensional Ring Stiffened Finite Length
Cylinder Subjected to a Pressure Pulse from 40 lbs PETN 30
Foot Standoff, Initial Mode 6 Imperfection $A_6 = 0.05h$ no phase
shift

Shock→
Wave
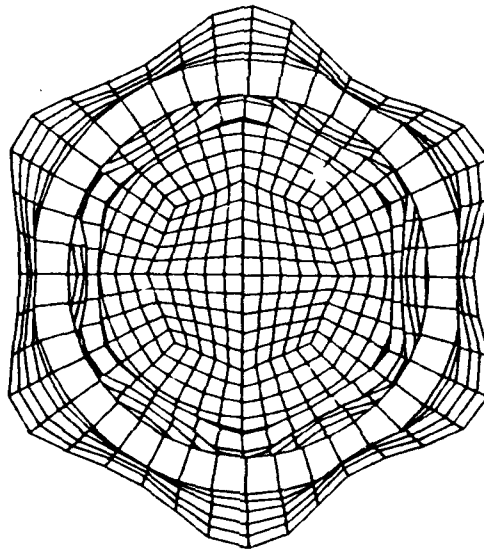
End View @ 5.0 ms

Figure 78. Three Dimensional Ring Stiffened Finite Length
Cylinder Subjected to a Pressure Pulse from 40 lbs PETN 30
Foot Standoff, Initial Mode 6 Imperfection $A_6 = 0.05h$ no phase
shift
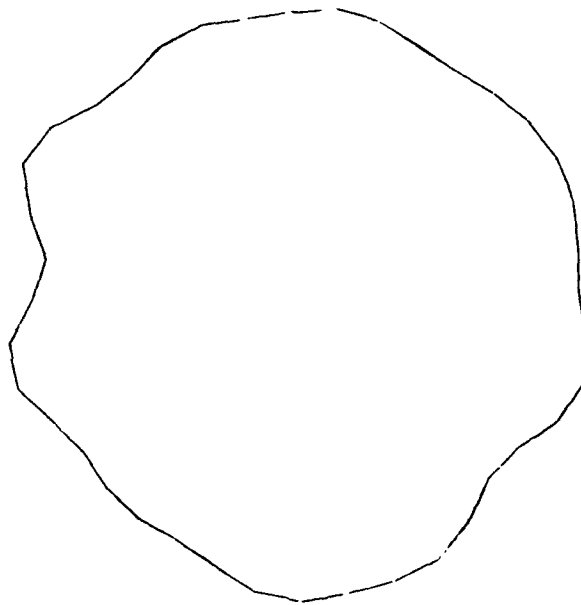
Initial Imperfection (imperfections scaled up 200X)

Figure 79. Three Dimensional Ring Stiffened Finite Length
Cylinder Subjected to a Pressure Pulse from 40 lbs PETN 30
Foot Standoff, Initial Imperfection First 10 modes $A_n = 0.01h$
with Random Phase Shift
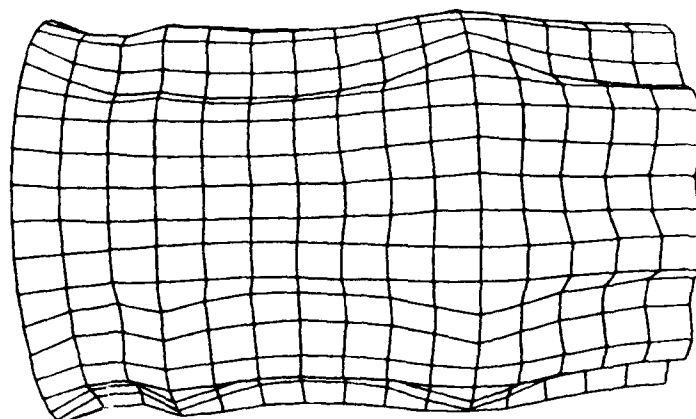
Front View @ 5.0 ms

Figure 80. Three Dimensional Ring Stiffened Finite Length
Cylinder Subjected to a Pressure Pulse from 40 lbs PETN 30
Foot Standoff, Initial Imperfection First 10 modes $A_n = 0.01h$
with Random Phase Shift

Shock→
Wave
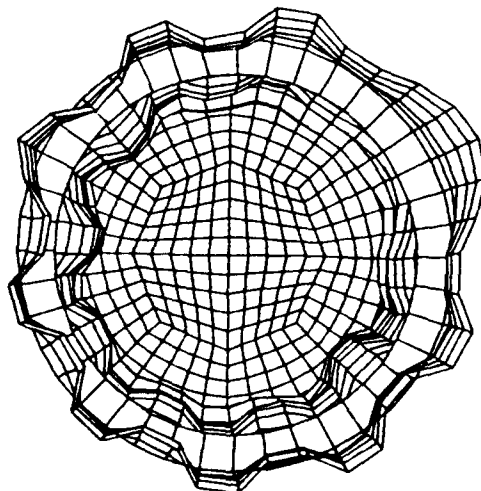
End View @ 5.0 ms

Figure 81. Three Dimensional Ring Stiffened Finite Length
Cylinder Subjected to a Pressure Pulse from 40 lbs PETN 30
Foot Standoff, Initial Imperfection First 10 modes $A_n = 0.01h$
with Random Phase Shift

VI. SUMMARY AND CONCLUSIONS

The response of test cylinders to underwater explosive shock is a complicated function of many factors.   One important factor that is often overlooked in the modeling of these underwater shock phenomena is the initial imperfections that are present in the test cylinders.   The response of model cylinders subjected to simulated underwater explosive shock has been shown to be very dependent to the initial imperfections introduced into the cylinder models.   The introduction of these imperfections not only caused the shape of the shell of the cylinder (as viewed from the end) to follow the shape of the initial imperfection but it has also changed the response of the shell near the endplates and stiffeners of the model cylinder.   The pinching of the shell near these stiffeners and endplates was greatly reduced or eliminated by the introduction of initial imperfections in the model cylinders.   This resulting response is closer to the response observed in test cylinders subjected to actual underwater shock loading.   In addition, the initial imperfections introduced increased the magnitude of the shell deformations compared to the deformations for cylinders modeled as perfect cylinders.

Changes in the cylinder geometry resulted in some changes in the response of the cylinder to underwater shock. However in all cases the introduction of initial imperfections greatly affected the response of the cylinder as compared to the response of a perfect cylinder.

If the initial imperfections of a test cylinder are known and introduced into a model cylinder used in finite element analysis, the results of the finite element analysis may more closely, simulate the actual response of the test cylinder.

FORTRAN PROGRAMS FOR MODIFYING INGRIDO FILE FOR MODAL
IMPERFECTIONS

```
      program imp
***********************************************************************
*   This program written by Donald T. Hooker II on 3/15/93   *
*   Revised 5/12/93                                          *
***********************************************************************
*   This program modifies the nodes of a file called        *
*   "ingrido.raw", which is an edited version of ingrido in  *
*   which the first line is the beginning of the node list.  *
*   This is one of a series of 2 programs, which need to be  *
*   run in order, i.e. "imp" then "convert".  These programs *
*   modify the node positions for modal imperfections WITH   *
*   OR WITHOUT random amplitudes and/or phase shifts.  The   *
*   final output file name is imp.dat.                       *
***********************************************************************
*   VARIABLE DECLARATION                                     *
*     a - angle from reference axis to radial position of    *
*       node                                                 *
*     a1 thru a10 - weighting factor for each modal          *
*       imperfection                                         *
*     b1 - ingrido constants                                 *
*     b2 - ingrido constants                                 *
*     dr - change in radial position due to modal            *
*       imperfections                                        *
*     dr1 thru dr10 - radial position change for each modal  *
*       imperfection                                         *
*     h - thickness of shell                                 *
*     n - node number                                        *
*     m - number of nodes                                    *
*     pi - 3.14159265359                                     *
*     ps1 thru ps10 - phase shift for each modal             *
*       imperfection                                         *
*     r - radial position of node                            *
*     randamp - if random amplitude is desired set randamp=1 *
*     randphs - if random phase is desired set randphs=1     *
*     x - x coordinate of node                               *
*     y - y coordinate of node                               *
*     z - z coordinate of node                               *
***********************************************************************

      double precision x,y,z,a,r,dr,h,pi
      double precision a1,a2,a3,a4,a5,a6,a7,a8,a9,a10
      double precision dr1,dr2,dr3,dr4,dr5,dr6,dr7,dr8,dr9,
```

```
     &  dr10
      double precision ps1,ps2,ps3,ps4,ps5,ps6,ps7,ps8,ps9,
     &  ps10
      integer randamp,randphs

*****************************************************************
*        OPEN INPUT AND OUTPUT FILES                           *
*****************************************************************

      open(14,file='ingrido.raw')
      open(15,file='imp.unconverted')

*****************************************************************
*        IF RANDOM MODE AMPLITUDE IS DESIRED SET RANDAMP EQUAL*
*        TO 1                                                  *
*        IF RANDOM MODE PHASE SHIFT IS DESIRED SET RANDPHS     *
*        EQUAL TO 1                                            *
*****************************************************************

      randamp = 0
      randphs = 1

*****************************************************************
*        INPUT NUMBER OF NODES TO BE MODIFIED AND WRITE NUMBER*
*        TO OUTPUT FILE IMP.UNCONVERTED                        *
*****************************************************************

      m = 921
      write(15,98)m
   98 format(1x,i5)

*****************************************************************
*        INPUT THICKNESS OF SHELL                             *
*****************************************************************

      h = 0.06

*****************************************************************
*        SET THE VALUE OF PI                                  *
*****************************************************************

      pi = 3.14159265359

*****************************************************************
*        INPUT THE WEIGHTING COEFFICIENTS OF THE FIRST TEN    *
*        MODE SHAPES                                          *
*****************************************************************

      a1 = 0.01
      a2 = 0.01
      a3 = 0.01
```

84

```
        a4 = 0.01
        a5 = 0.01
        a6 = 0.01
        a7 = 0.49
        a8 = 0.64
        a9 = 0.81
        a10 = 1.0


*******************************************************************
*       INPUT PHASE SHIFT FOR EACH MODE SHAPE                     *
*******************************************************************

        ps1 = 0.0
        ps2 = 0.0
        ps3 = 0.0
        ps4 = 0.0
        ps5 = 0.0
        ps6 = 0.0
        ps7 = 0.0
        ps8 = 0.0
        ps9 = 0.0
        ps10 = 0.0


*******************************************************************
*       INPUT SEED NUMBER FOR RANDOM NUMBER GENERATOR             *
*******************************************************************

        seed = 1.0


*******************************************************************
*       CALL SUBROUTINE SRAND TO GENERATE SEED NUMBER FOR         *
*       RANDOM NUMBER GENERATOR SUBROUTINE                        *
*******************************************************************

        call srand(seed)


*******************************************************************
*       CALL SUBROUTINE RAND TO GENERATE RANDOM PHASE SHIFT       *
*       FOR EACH MODE SHAPE                                        *
*******************************************************************
        if (randphs .eq.1) then
          ps1 = 2. * pi * rand()
          ps2 = 2. * pi * rand()
          ps3 = 2. * pi * rand()
          ps4 = 2. * pi * rand()
          ps5 = 2. * pi * rand()
          ps6 = 2. * pi * rand()
          ps7 = 2. * pi * rand()
          ps8 = 2. * pi * rand()
          ps9 = 2. * pi * rand()
          ps10 = 2. * pi * rand()
```

85

```
          endif

***********************************************************************
*        CALL SUBROUTINE RAND TO GENERATE RANDOM WEIGHTING OF *
*        MODE SHAPES                                          *
***********************************************************************

          if (randamp .eq. 1) then
            a1 = a1 * rand()
            a2 = a2 * rand()
            a3 = a3 * rand()
            a4 = a4 * rand()
            a5 = a5 * rand()
            a6 = a6 * rand()
            a7 = a7 * rand()
            a8 = a8 * rand()
            a9 = a9 * rand()
            a10 = a10 * rand()
          endif

***********************************************************************
*        DO LOOP TO READ INPUT DATA                          *
***********************************************************************

          do 100 i=1,m
            read(14,*) n,b1,x,y,z,b2

***********************************************************************
*        CALCULATE RADIUS OF NODE POSITION                    *
*        (Look carefully at the axis of rotation of the       *
*        cylinder to determine the proper Cartesian           *
*        coordinates used to calculate the radius of the      *
*        cylinder.  In this case the axis of rotation is the z*
*        axis.                                                *
***********************************************************************

          r=(x*x+y*y)**0.5

***********************************************************************
*        CALCULATE THE ANGLE FROM THE REFERENCE AXIS TO THE   *
*        NODE POINTS (Look carefully at the zero angle        *
*        direction.  In this case the x axis points in the    *
*        direction of the charge.)                            *
***********************************************************************

          if ((dabs(y).lt. 0.001)) then
            if (x.gt.0.0) then
              a=0.0
            else
              a=pi
            endif
```

86

```fortran
          else
            a=datan(y/x)
            if (x.lt.0.0) then
              a=a+pi
            endif
          endif


**************************************************************
*      MODIFY THE NODE POSITIONS USING THE FIRST TEN MODE    *
*      SHAPES                                                 *
**************************************************************

          dr1 = a1 * h * dcos(a + ps1)
          dr2 = a2 * h * dcos(2. * a + ps2)
          dr3 = a3 * h * dcos(3. * a + ps3)
          dr4 = a4 * h * dcos(4. * a + ps4)
          dr5 = a5 * h * dcos(5. * a + ps5)
          dr6 = a6 * h * dcos(6. * a + ps6)
          dr7 = a7 * h / 7. / 7. * dcos(7. * a + ps7)
          dr8 = a8 * h / 8. / 8. * dcos(8. * a + ps8)
          dr9 = a9 * h / 9. / 9. * dcos(9. * a + ps9)
          dr10 = a10 * h / 10. / 10. * dcos(10 * a + ps10)
          dr = dr1 + dr2 + dr3 + dr4 + dr5 + dr6 + dr7 + dr8 +
     &       dr9 + dr10


**************************************************************
*      CALCULATE THE CARTESIAN COORDINATES OF THE NODES      *
**************************************************************

          x=x-dr*dcos(a)
          y=y-dr*dsin(a)


**************************************************************
*      WRITE DATA TO TEMPORARY DATA FILE IMP.UNCONVERTED     *
**************************************************************

          write(15,998) n,b1,x,y,z,b2
  998     format(i8,f5.0,3e20.13,f5.0)
  100 continue


**************************************************************
*      CLOSE INPUT AND OUTPUT FILES                          *
**************************************************************

          close(14)
          close(15)
          stop
          end
```

```
      program convertimp

*****************************************************************
*   This program written by Donald T. Hocker II on 3/15/93    *
*   Revised 3/30/93                                           *
*****************************************************************
*   This program converts numerical data
from"imp.unconverted"*
*   into ascii format for use in modifying ingrido for modal*
*   imperfections                                            *
*****************************************************************
*   VARIABLE DECLARATION                                     *
*      f* - data to be converted to ascii format            *
*      m - number of nodes                                  *
*****************************************************************

      character*13 f1
      character*1 f2,f3,fz
      character*18 f4
      character*1 f5,f6
      character*18 f7
      character*1 f8,f9
      character*18 f10
      character*5 f11
      open(14,file='imp.unconverted')
      open(15,file='imp.dat')
      fz='0'

*****************************************************************
*     READ NUMBER OF NODES TO BE MODIFIED                    *
*****************************************************************

      read(14,*) m

*****************************************************************
*     DO LOOP TO READ DATA AND CONVERT IT TO ASCII FORMAT    *
*****************************************************************

      do 100 i=1,m
        read(14,998)f1,f2,f3,f4,f5,f6,f7,f8,f9,f10,f11
  998   format(a13,a1,a1,a18,a1,a1,a18,a1,a1,a18,a5)
        write(15,998)f1,f3,fz,f4,f6,fz,f7,f9,fz,f10,f11
  100 continue

*****************************************************************
*     CLOSE INPUT AND OUTPUT FILES                           *
*****************************************************************
      close(14)
      close(15)
      stop
      end
```

APPENDIX B

INGRID INPUT FILE FOR TWO DIMENSIONAL INFINITE CYLINDER MODEL

```
INFINITE CYLINDER MODEL
dn3d vec term 5.0e-3 plti 1.0e-5 prti 1000.

mat 1 type 3 e 2.9e+7 pr 0.3 ro 7.356e-4
    etan 5.1e+4 sigy 3.2e+4 shell quad 5 thick 0.060 endmat

lcd 1 2 0.0 0.0 1.0 0.0
lcd 2 2 0.0 2.5e-8 1.0 2.5e-8


plan 2

 0 0 -.003    0  0 -1  0.001   symm
 0 0  .003    0  0  1  0.001   symm

start

 -1   6   -11 ;
 -1   6   -11 ;
  1 2 ;
 -1.  0.  1.
 -1.  0.  1.
 -.003  .003
 a 1 1 0 3 3 0 3 6.0
 pri -1 -3 ; -1 -3 ; ; 1 -1.0 0. 0. 0.
 mate 1
end
end
```

APPENDIX C

MATERIAL MODEL DETAILS

For the steels used in the numerical models, a bilinear stress-strain type model was used. The material model used was a "Kinematic/Isotropic Elastic Plastic" model (Hallquist 1990). Figure 82 shows a typical stress-strain diagram for the materials used. A hardening parameter of 0, giving pure kinematic hardening, was used for all of the steels. Strain rate hardening was not used for the materials in this study.

Typical properties of the materials used in the numerical models are:

		Mild Steel	HY-100
Density(ρ)	(lb_m/ft^3) :	490	490
Poission's Ratio(ν)	:	0.3	0.3
Yield Stress(σ_y)	(psi) :	3.2×10^4	1.08×10^5
Young's Modulus(E)	(psi) :	2.9×10^7	2.9×10^7
Hardening Modulus(E_{tan})	(psi) :	5.1×10^4	5.02×10^4

For the deformations encountered in this study the materials did not approach their fracture stress.
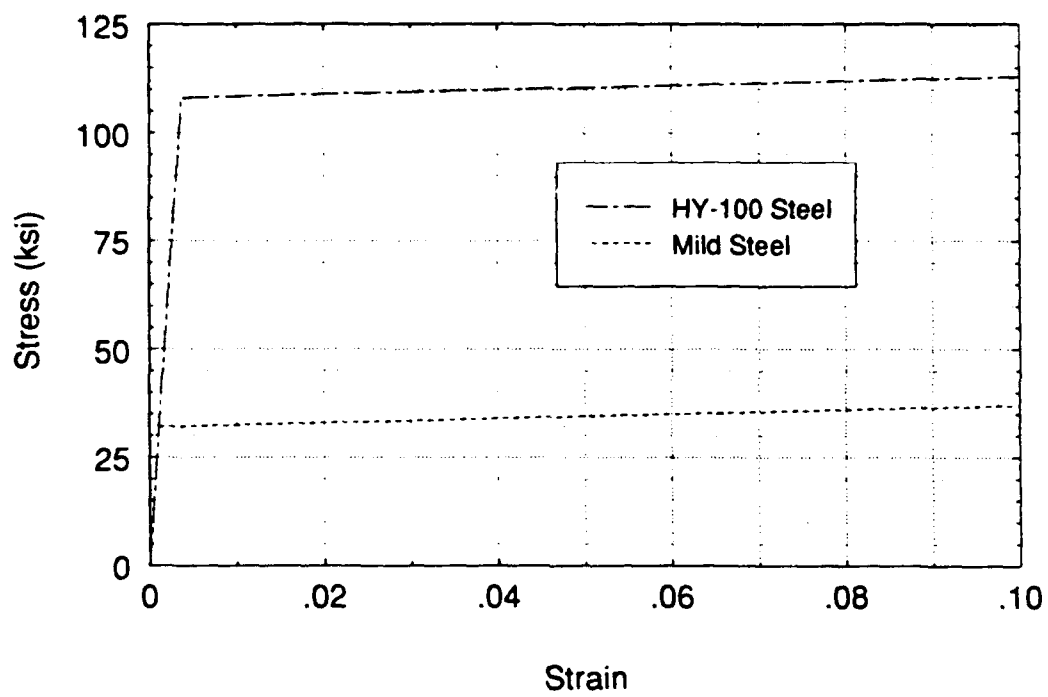
Figure 82.   Typical Bilinear Stress-Strain Diagram

APPENDIX D

INGRID INPUT FILE FOR THREE DIMENSIONAL STIFFENED INFINITE CYLINDER MODEL

```
STIFFENED INFINITE CYLINDER MODEL
dn3d vec term 5.0e-3 plti 1.0e-5 prti 1000.

c
c       material definitions
c
c       shell material (mild steel)
c

 mat 1 type 3 e 2.9e+7 pr 0.3 ro 7.356e-4
     etan 5.1e+4 sigy 3.2e+4 shell quad 5 thick 0.060 endmat
c
c       stiffener material (mild steel)
c

 mat 2 type 3 e 2.9e+7 pr 0.3 ro 7.356e-4
     etan 5.1e+4 sigy 3.2e+4 shell quad 5 thick 0.12 endmat

c
c       load curve definitions
c

lcd 1 2 0.0 0.0 1.0 0.0
lcd 2 2 0.0 1.0e-6 1.0 1.0e-6

c
c       symmetry planes
c

plan 2

 0 0 -6.     0  0 -1  0.001  symm
 0 0  6.     0  0  1  0.001  symm
c
c       construct shell
c

start

 -1  11  -21 ;
 -1  11  -21 ;
  1   6  11 ;
```

```
 -1.   0.   1.
 -1.   0.   1.
 -6.   0.  6.
 a 1 1 0 3 3 0 3 6.0
 pri -1 -3 ; -1 -3 ; ; 1 -1.0 0. 0. 0.
 mate 1
end
c
c       construct stiffener
c

start

1 2 12 22 23 ;
1 2 12 22 23 ;
-1 ;
-1 -1 0 1 1
-1 -1 0 1 1
0
di 1 2 0 4 5 ; 1 2 0 4 5 ; ;
a 1 1 0   5 5 0   3 6.0
a 2 2 0   4 4 0   3 5.0
d 2 2 0 4 4 0
mate 2
end
end
```

INGRID INPUT FILE FOR THREE DIMENSIONAL STIFFENED FINITE
CYLINDER MODEL

```
STIFFENED FINITE CYLINDER
dn3d vec term 5.0e-3 plti 1.0e-5 prti 1000.

c       material definitions
c       shell material (mild steel)

 mat 1 type 3 e 2.9e+7 pr 0.3 ro 7.356e-4
      etan 5.1e+4 sigy 3.2e+4 shell quad 5 thick 0.060 endmat
c
c       stiffener material (mild steel)
c

 mat 2 type 3 e 2.9e+7 pr 0.3 ro 7.356e-4
      etan 5.1e+4 sigy 3.2e+4 shell quad 5 thick 0.12 endmat

c       endplate material (HY-100 steel)

 mat 3 type 3 e 2.9e+7 pr 0.3 ro 7.356e-4
      etan 5.02e+4 sigy 1.08e+5 shell quad 5 thick 0.25
endmat

c
c       load curve definitions
c

lcd 1 2 0.0 0.0 1.0 0.0
lcd 2 2 0.0 1.0e-6 1.0 1.0e-6

c
c       symmetry planes
c

plan 1

 0 0  0.0    0  0 -1  0.001  symm

c
c       construct shell
c

start
 -1  6  -11 ;
```

```
   -1   6   -11  ;
    1       16  ;
   -1.   0.   1.
   -1.   0.   1.
    0.0     18.0
  a 1 1 0 3 3 0 3 6.0
  pri -1 -3 ; -1 -3 ; ; 1 -1.0 0. 0. 0.
  mate 1
 end

 c
 c       construct stiffener
 c

 start

 1 2 7 12 13 ;
 1 2 7 12 13 ;
 -1 ;
 -1 -1 0 1 1
 -1 -1 0 1 1
 6.0
 di 1 2 0 4 5 ; 1 2 0 4 5 ; ;
 a 1 1 0   5 5 0   3 6.0
 a 2 2 0   4 4 0   3 5.0
 d 2 2 0 4 4 0
 mate 2
 end

 c
 c       construct endplate
 c       surface definitions
 c
 sd 1 cyli 0 0 0   0 0 1    6.0
 sd 2 cyli 0 0 0   0 0 1   [6.0*3/5]

 start
  1 5 10 15 19 ;
  1 5 10 15 19 ;
 -1 ;
 -1 -1 0 1 1
 -1 -1 0 1 1
 18.0
 pr 1 1 1   5 5 1   1   -1.0   0.0 0.0 0.0
 di 1 2 0 4 5 ; 1 2 0 4 5 ; ;
 sfvi -2 -4 ; -2 -4 ; ; sd 2
 sfi -1 -5 ; -1 -5 ; ;   sd 1
 mate 3
 end
 end
```

REFERENCES

Arbocz, J. (1982). "The Imperfection Data Bank, A Means to Obtain Realistic Buckling Loads." In *Buckling of Shells, Proc. of a State-of-the-Art Colloquium*, New York, N.Y.

Belytschko, T. B. and Tsay, C. S. (1984). "Explicit Algorithms for Nonlinear Dynamics of Shells." *Comp. Meth. Appl. Mech. Eng.*, 43, pp. 21-276.

Chisum, J. E. (1992). *Response Predictions for Double Hull Cylinders Subjected to Underwater Shock Loading*. Engineer's Thesis, Naval Postgraduate School, Monterey, CA.

Fox, P. K. (1992) *Nonlinear Dynamic Response of Cylindrical Shells Subjected to Underwater Side-on Explosions*. Master's Thesis, Naval Postgraduate School, Monterey CA.

Hallquist, J. O., and Stillman, D. W. (1990). "VEC/DYNA3D Users Manual (Nonlinear Dynamic Analysis of Structures in Three Dimensions)." Livermore Software Technology Corporation Report 1018.

Hughes, T. J. R., Liu, W. K., and Levitt, I., (1981). "Nonlinear Dynamics Finite Element Analysis of Shells." *Nonlinear Finite Element Analysis in Struct. Mech.*, Eds. W. Wunderlich, E. Stein and K. J. Bathe, Springer-Verlag, Berlin, pp. 151-168.

Kirkpatrick, S. W., and Holmes, B. S. (1989). "Effect of Initial Imperfections on Dynamic Buckling of Shells." *Journal of Engineering Mechanics*, v. 115, pp. 1075-1093.

Lindeberg, H. E., and Florence, A. L. (1987). *Dynamic Pulse Buckling*. Martinus Nijhoff Publishers, Dordrecht, The Netherlands.

INITIAL DISTRIBUTION LIST

No. of Copies

1. Defense Technology Information Center   2
   Cameron Station
   Alexandria, Virginia 22304-6145

2. Library, Code 52   2
   Naval Postgraduate School
   Monterey, California 93943-5002

3. Professor Y. S. Shin, Code ME/Sg   2
   Department of Mechanical Engineering
   Naval Postgraduate School
   Monterey, California 93943

4. Professor Y. W. Kwon, Code ME/Kw   1
   Department of Mechanical Engineering
   Naval Postgraduate School
   Monterey, California 93943

5. Naval Engineering Curricular Office   1
   Code 34
   Naval Postgraduate School
   Monterey, California 93943-5000

6. Dr. Kent Goering   1
   Defense Nuclear Agency
   6801 Telegraph Road
   Alexandria, Virginia 22310

7. Mr. Douglas Bruder   1
   Defense Nuclear Agency
   6801 Telegraph Road
   Alexandria, Virginia 22310

8. Dr. Roshdy S. Barsoum   1
   Office of Naval Research
   Mechanics Division, Code 1132
   800 North Quincy Street
   Arlington, Virginia 22217-5000

9. LT Donald T. Hooker II, USN   1
   4155 Boomer Rd.
   Cincinnati, Ohio 45247

10. Dr. Benjamin Whang   1
    Carderock Division
    Naval Surface Warfare Center
    Code 67-1
    Bethesda, Maryland 20084-5000

11. Mr. Michael Riley   1
    Naval Surface Warfare Center
    UERD
    Portsmouth, Virginia 23709-5000

12. Mr. Mike Talley   1
    Naval Surface Warfare Center
    UERD
    Portsmouth, Virginia 23709-5000